MEASUREMENT OF CORRELATION COEFFICIENT OF ANGLE DIVERSITY SIGNALS IN TROPOSCATTER SYSTEMS

A Thesis Submitted
In Partial Fulfilment of the Requirements
for the Degree of
MASTER OF TECHNOLOGY

By

R. C. PANDEY

to the
DEPARTMENT OF ELECTRICAL ENGINEERING
INDIAN INSTITUTE OF TECHNOLOGY, KANPUR
DECEMBER, 1979

CERTIFICATE

Certified that this work, 'Measurement of Correlation Coefficient of Angle Diversity Signals in Troposcatter Systems' by Mr. R.C. Pandey has been carried out under our supervision and that this has not been submitted elsewhere for a degree.

Dec. 7,1979

(K.R. SARMA)
Professor

(P.R.K. RAO)
Professor

Department of Electrical Engineering
Indian Institute of Technology
KANPUR

EG-1979-M-PAN-MEA

ACKNOWLEDGEMENT

I am highly thankful to Prof. K.R. Sarma and Prof. P.R.K. Rao for their encouragement, assistance and expert guidance during the course of this project. I also wish to express my gratitude to Prof. N.C. Mathur and Prof. K.C. Gupta for their valuable technical advise.

I shall cherish the memory of my interesting technical discussions with Sri Bh. A.R.B. Raju, Research Engineer, A.C.E.S., which were very much useful during system development work. I am thankful to him for his valuable assistance in data logging operation during the night hours. I am thankful to Dr. Mahra of U.P. State Observatory, Naini Tal for providing timely transmissions from Naini Tal at short notice. Thanks are also due to Sri Arjun Raman, Sri D.K. Trivedi, Sri S. Manoharan and Sri K.S. Ananthakrishnan, Research Engineers in ACES for their help at various stages of system development and to Mr. Waryam Singh, Programmer, for his assistance in working on IBM 1800.

I am grateful to my wife for her efficient handling of all family problems during this period, leaving me free to concentrate on my studies. I am also thankful to the Director, D.T.D. and P (Air), for having provided me this opportunity of improving my academic qualifications.

ABSTRACT

Signals received over a troposcatter communication channel are characterised by severe fading. To mitigate the effects of short term fading, space diversity or frequency diversity techniques are normally used. This study has been undertaken to explore the feasibility of utilising angle diversity as an economic and workable alternative.

An experiment has been conducted to determine the correlation coefficient between tropo signals received from two common volumes, which are at different elevation angles with respect to the receiver. An existing 2.1 GHzs experimental link between Kanpur and Nainital has been used for the experiment after incorporating an additional feed horn, laterally displaced with respect to the existing feed horn, to obtain the elevated beam.

The receiver used is ofdouble superheterodyne type, using coherent A.M. detection scheme, the reference signal being provided by a P.L.L. The input of this receiver is switched between two horns, every 50 ms. Receiver output is sampled synchronously using an IBM 1800 computer. 1 minute samples are stored in magnetic tape in digital form.

Results of experiment indicate that the signals received over the two paths exhibit low correlation necessary for effective diversity gain.

TABLE OF CONTENTS

CHAPTER 1

INTRODUCTION

1.1 Fading in Tropo Communication Systems:

One of the significant achievements in the field of communications since the end of World war II has been the utilisation of tropo-scatter propogation for long range point to point communication systems in the frequency range of 400 MHzs to 8000 MHzs. With the aid of this mode of propogation, it is possible to communicate reliably between distant points, seperated by rugged terrain, water barriers or enemy territory, several hundred miles away.

Scatter signal at a particular instant appears to be the resultant of a number of individual signals arriving with random phase differences. Over a period of time, the random variations of phase produce a signal of varying amplitudes which has been termed as fading.

There are two general classes of fading associated with tropospheric scattering namely 'fast fading' and 'slow fading'. The slow or long term fading results from gross changes in atmospheric conditions, changes which take place on a diurnal and seasonal basis. It is common practice to obtain the cumulative distribution of the random signal amplitude over an hourly period and to express

these slow variations in signal level in terms of variations of the hourly median value. Statistical distributions of the signal amplitude approaches a log normal distribution for hourly periods.

Superimposed on the long-term signal variations is a rapid and intense fading characteristic. This fast fading occurs because the total received signal is the phasor sum of many signals coming from different blobs in the atmosphere. Since these blobs are in constant turbulent motion, the compound signals have a range of amplitudes and their phase relationship is random. The statistical distribution of the signal amplitude is approximately a Rayleigh distribution for periods of a few minutes. Results of many investigators tend to indicate that a one minute sampling period seems to give almost a perfect Rayleigh distribution [1]. The characteristic time of the fast fades may be as short as 0.1 secs.

1.2 Diversity Techniques to overcome the Effect of Fading:

While the effects of long term fading have to be taken into account by giving suitable fade margins during the system design, effects of fast fading can be mitigated by using diversity reception. A system is designed to operate for a given percentage of time above a certain

specified signal to noise level. By using diversity reception, we can get two or more uncorrelated signals at the receiver input and decrease the time that the signal spends at low levels by suitably combining these uncorrelated signals using either predetection or post-detection combining techniques.

Usefulness of diversely in overcoming the effects of rapid fading is well established. The basic requirements for successful utilisation of this technique are two fold. First is the independence of fading between various diversity channels. This means that the cross-correlation coefficient should be low preferably under 0.4 for it has been shown that coefficients as high as 0.6 cause only negligible deterioration of the reliability level achieveable with zero cross-correlation between channels. The second requirement for successful diversity operation is that the various diversity channels contribute an approximately equal amount of average power to the combined sum.

Typical diversity techniques include space diversity, frequency diversity, polarisation diversity, angle diversity and time diversity. Most prevelent of these is space diversity. In space diversity, two or more receiving antennas are spaced at about 100 wavelengths, perpendicular

to the great circle path between transmitter and receiver. Two fold or four fold space diversity configurations or four fold space-frequency diversity configurations are most commonly used.

Space diversity, although highly effective, can become prohibitively expensive as additional antennas are added. While frequency diversity requires only one antenna at each end, it is very expensive in terms of the number of transmitters and frequency spectrum required. Polarisation diversity fails to produce the relative independence required while time diversity results in considerable equipment complexity.

Angle diversity (AD) is an alternative to space frequency or can supplement it to increase the order of diversity. Additional feed horns provide additional beams on each antenna. With feed horns touching, the beams are in close proximity but their 3 db common volumes are distinctly separated and cover different atmospheric regions. It has been reported [7] that AD signals have very low short-term correlation and also usefully low correlation (about 0.5) of medians over periods of 5 minutes to several hours. The median on an upper signal were frequently stronger than or comparable with the main beam median. Moreover a weaker upper beam

signal was often less correlated by multipath distortion and more useful than the main beam signal.

The importance of angle diversity increases sharply as the operating frequencies are increased to S.H.F. range. To maintain the desired level of communication reliability it is necessary to increase either the antenna size or the order of diversity or both. Increasing the antenna size alone is not particularly efficient at S.H.F. frequencies, since the accompanying increase in the aperture to medium coupling loss prevents realisation of antenna gains proportional to the antenna aperture. Increasing the order of diversity by using additional antennas as in space diversity or combining of space and frequency diversity have produced a workable but costly solution. Angle diversity provides a workable and economic alternative at these frequencies as it saves the cost of additional large antenna structures or high power transmitters.

1.3 Review of Early Experimental Work:

A series of experiments were conducted by Crawford [2] on a 176 mile overland path between Pharsalia New York and Crawford Hill, New Jersey during the period May 55 - Sept. 58 using xmitting antennas of 10' and 28' diameter and receiving antennas of 28' and 60' diameter. Experiments

were conducted at 460 MHzs and 4110 MHzs, using both vertically and horizontally displaced feed horns. Recording of signals was done by using a two channel 'Sanborn Recorder'. Level distribution counters were used to totalise the time, the signal was below a preset level and coincidence counters were used to detect the number of times when both channels were below a common preset level.

The percentage time the amplitude of switched signal should spend below the level where the counter was set (if signals were uncorrelated and Rayligh distributed) was computed using theoritical curves and compared with the percentage time the switched channel actually spends below the setting. Experimental points were found to fall on both sides of theoritical curves due to experimental inaccuracies.

Vogelman, Ryerson and Bickelhart [3]reported an experiment during the same period. They used an existing RADC link between Mount Rose and Forest Port, a distance of slightly more than 200 miles operating at a frequency of 7630 and 8450 MHzs. A 6' diameter dish was used with a 2 KW transmitter at Mount Rose site. The receiving antenna was a 28' dish. An assembly of four feeds was made with three feeds in a row and the fourth feed above the central feed. The outer feeds of the row of three were positioned

at a distance from central feed, which produced a beam scan of about 3 beam-widths. The feed above the row of three was positioned to provide a beam scan of 3 beamwidths in the vertical plane.

Data were recorded on two beams at a time for each of the six possible combinations. Data were collected in two groups. Firstly signal level information was obtained directly from the IF strips on two receivers. Secondly teletype signals were received and recorded at the video output of each receiver. Greatest correlation obtained was 18.4%.

Davis Surenian [4] used a 170 mile long experimental system between Model city N.Y and Verona N.Y. The transmitting station at Model city had a 28' parabolic dish with seven feeds, each feed fed independently by a 2 KW transmitter. Receiving station was equipped with two antennas similar to the transmitting antenna, each resolving seven beams. The resulting fourteen receiving channels were independently amplified and filtered to seperate the different carriers and coherently combined in an equal gain predetection combiner. Feeds were so placed that the -3 db contours of associated beams touched each other. Xmitting channels operated in three different modes.

i) T_1 mode - Single x mitter channel was operated.

ii) T_2 mode - Two or more channels were operated all at the same frequency.

iii) T_3 mode - Two or more channels operated at different frequencies spaced 1 or 2 MHzs. apart.

Correlation coefficient between various pairs of beams under various transmitter modes were measured and compared with measured correlations in space diversity mode. The analysis of experimental results showed that with n fold angle diversity operation, diversity improvement comparable to that obtained by the use of n-space diversity channels (which would require n antennas) is possible. It was shown that most successful operation is achieved with a single, narrow transmitting beam illuminating the troposphere and a group of equally narrow receiving beams, all operating at the same frequency, receiving energy from this region of troposphere.

More recently Monsen [5] conducted an experiment using a 288 Km. link between Monrovia and Grawford Hill, at a frequency of 2170 MHzs. with a 28' transmitting antenna dish, 60' receiving antenna dish and a horn feed arrangement that produced three vertical angle diversity beams and three horizontal angle diversity beams. Long term data was

collected using a xmitted pseudo random PSK signal operating at either 0.5 or 1 M bit/sec. This allowed measurement of both channel characteristics as well as error rate performance.

Received signals were envelope detected and logarithmically amplified. A PDP-8L computer with an AX-08 peripheral unit sampled and performed an A/D conversion every 100 ms. 10 min. histograms of signal strengths of all horns were developed by computer and correlation coefficient was computed for that period. Results show that the vertical angle diversity combinations exhibit the low correlation necessary for effective diversity gain.

1.4 Scope of the Experiment:

The experiment was undertaken with a view to confirm the findings of the earlier experiments that there is a low correlation coefficient between tropo signals arriving at a receiver after scattering from two common volumes which are at different elevation angles with respect to each other. Elevated beam was provided by using an additional feed horn laterally displaced with respect to the existing main horn.

CHAPTER 2

EXPERIMENTAL SET UP

2.1 System Design Considerations:

The existing experimental tropo link between Kanpur and Nainital was utilised to carry out the experiment. Salient features of the link are given in Table 1.

TABLE 1

Kanpur Nainital Tropo Link

Great circle distance	- 325.75 km
NS	- 290
Freq. of operation	- 2.1 GHzs.
Scatter angle	- .635°

Transmitting System		Receiving System	
U.P. State Observatory, Nainital		Indian Institute of Technology Kanpur	
Altitude	- 6150'	Altitude	- 415'
Latitude	- 26°-30'-56"	Latitude	- 29°-21'-38.9"
Longitude	- 80°-14'-10"	Longitude	- 79°-27'-25.6"
Parabolic Antenna dia	- 28'	Parabolic Antenna dia	- 28'

A block schematic of the system set up as it existed at the time of taking up of project is given in Fig. 2.1(a).

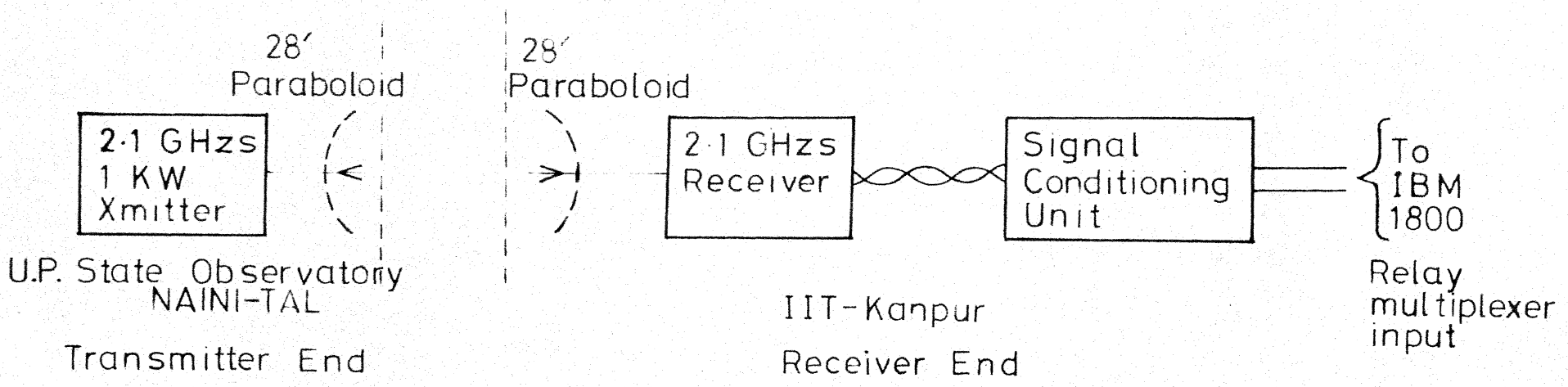

Fig. 2·1 a Block Diagram - Original System

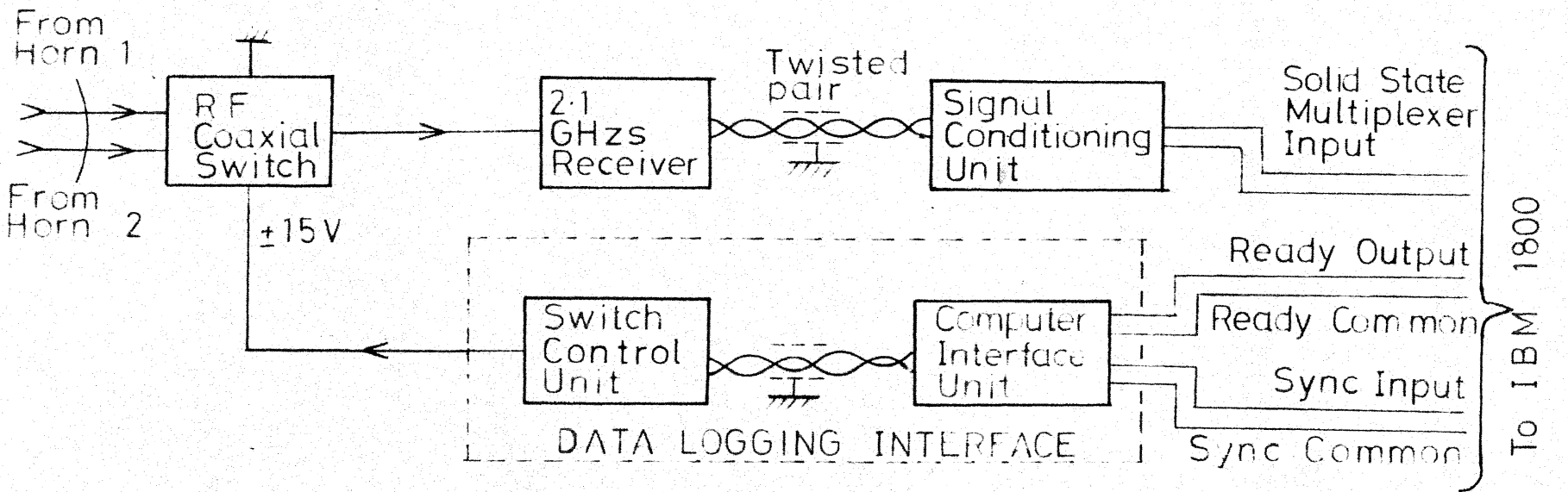

Fig. 2·1 b Block Diagram - Modified System (Receiver End)

Modifications were made to the antenna system for obtaining signals from two different 'common volumes'. An additional feed horn displaced lateraly with respect to the existing horn, was used to provide an elevated beam. The two receiving beams intersected the transmitted beam at different regions of atmosphere, therefore the signals received by two horns could be considered as being received by scattering from different common volumes.

The receiving system also needed modification as signals received from two horns had to be processed so that correlation between the two signal levels could be found out. An ideal solution would have been to have two parallel receiving chains and to sample the signals from two horns to find out the instantaneous signal levels at the same instant of time. However fabrication of an additional receiver was not possible within the available time frame and infra-structure.

The second alternative was to utilise the existing receiver but to carry out multiplexing of signals from two horns, at the input to the receiver. The receiver output in this case was a slowly changing D.C., within each switching interval, with sudden changes of level after each switching interval depending on the r.f. signal

levels at the two horns. Samples were taken from the receiver output, once within each switching interval. If the switching between two horns was done at a sufficiently fast rate, the signals from each horn could be reconstructed.

Taking into account the available time frame, the second alternative was chosen. The rate at which multiplexing could be done was limited by two factors. The first was the finite switching time of the r.f. switch used. The r.f. coaxial switch that could be obtained, had a nominal switching speed of 35-50 ms. To obtain a reliable long term operation a switching speed of 50 ms was choosen. This implied that each horn was connected to the receiver 10 times/sec. and 10 samples/sec could be taken. The second factor was the capabily of the phase locked loop to keep its lock as the signal was switched between two horns at a fast rate. Since the loop is used as a tracking filter, the output of the phase detector is a beat note between the received signal and the VCO frequency. For fading signals this beat note is deeply embedded in noise, and a narrow bandwidth filter is needed to recover it. The lock up transient, however occupies a time of the order of $\frac{1}{\omega_n}$ seconds. ω_n is of the order of 2 B_L where B_L = one sided loop noise bandwidth and is 160 cycles for our receiver. Thus the time required to lock

is of the order of 3 ms, which is well within the 25 ms time at which the sample is taken from the receiver output, after a horn has been switched to the receiver input. A second order loop with an active filter has the additional advantage of a large memory and therefore a longer holding time in the event of a signal drop out.

A sampling rate of 10 times/sec. for each horn meant that the system was capable of reconstruction of signal envelopes varying up to a maximum of 5 cycles per second. For high fading rates aliasing may take place. Past experience had however shown that the fading rates generally observed were of the order of 50 to 70 fades/min, [19] although higher fading rates up to 10 fades/sec. have been occassionally reported in cases of unsual turbulance of the type caused by an aircraft passing through the common volume. A sampling rate of 10 samples/sec. was therefore considered satisfactory for the purpose of our experiment.

Suitable data logging interface was designed, so that sampling of receiver output was carried out in synchronism with the switching action of the r.f. switch, taking into account the settling time of the switch. A block diagram of the modified system is given in Fig. 2.1(b).

2.2 Transmitting System:

This consists of a 1W drive unit, which is capable of giving a power output of 1W at 2.1 GHzs. The output of this unit is connected through a variable attenuator to the input of a multicavity klystron amplifier, which delivers a power output of 1 KW to the antenna system.

2.2.1 1W Drive Unit:

Block diagram of 1W drive unit is given in Fig. 2.2. A crystal oscillator (ON-1001) gives an output of +5 dbm at 29.167 MHzs. The oscillator output is fed to a limiter amplifier (BN-1012) giving an output of +20 dbm. The transistor tripler (BN-1009) which is also incorporated in the same unit gives an output of +24 dbm at 87.5 MHzs.

A transistor doubler, power amplifier and a varactor doubler (BM-1008) multiply the signal to 175 MHzs. The power amplifier output is 9.5 W at 175 MHzs.

The varactor tripler (ON-1003) converts it to 525 MHzs and gives a power output of 3.5 W at this frequency. Two stages of varactor doublers (OQ-1005 and OQ-1006) follow giving a power output of 1W at 2-1 GHzs. This is fed to the output connected through a 30 db directional coupler (HS-1002) and an isolator.

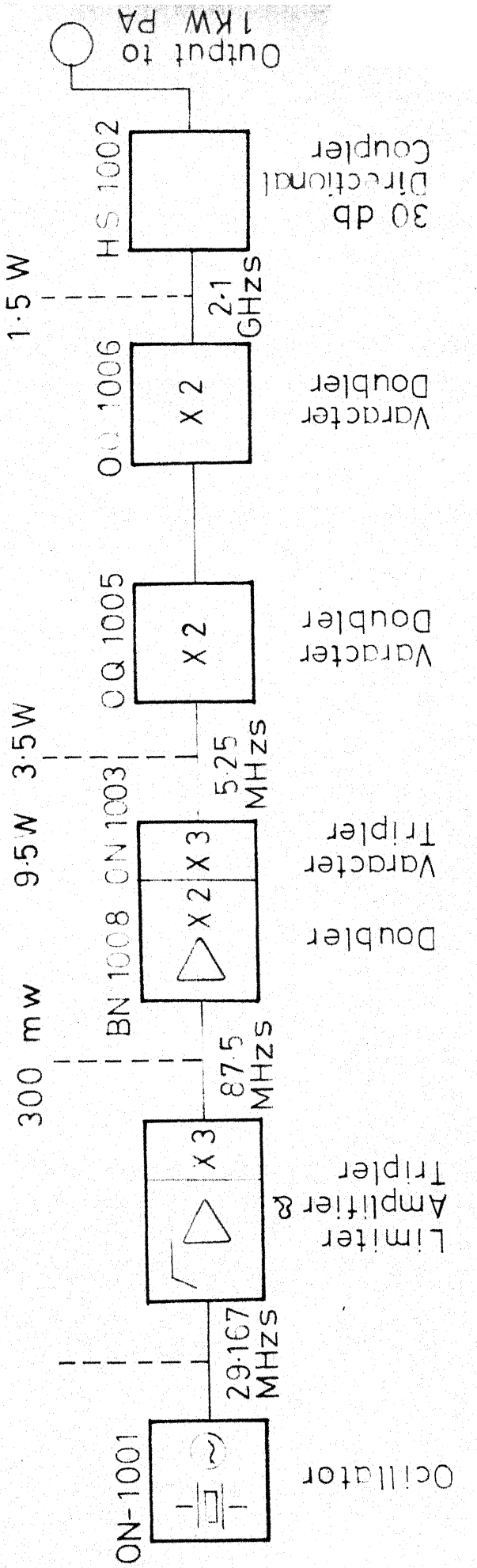

Fig. 2·2 2·1 GHzs Drive Unit Block Diagram

2.2.2 1 KW Power Amplifier:

A schematic diagram of 1 KW power amplifier is shown in Fig. 2.3. This uses an aircooled Klystron tube $4K_3SJ$ requiring a nominal $\angle^{\text{voltage}}$ of 6 KV at 400 mA to deliver the rated r.f. power output of 1 KW. The required beam voltage is generated within the amplifier using a regulated 3 phase 400 volt supply. Beam voltage can be manually adjusted by a variac to provide reduced power operation. Suitable control circuitry has been provided so that beam voltage can not be applied to klystron unless the air flow switch has operated and 3 minutes have elapsed after application of filament voltage. Protection has been provided against beam current overload and reflected power overload.

The amplified RF signal passes through a filter and directional coupler to the antenna system through a $1\frac{5}{8}$" coaxial cable.

2.3 Antenna System:

Antenna system consists of a transmitting and a receiving antenna, both being parabolic reflectors of 28' diameter aperture with 12.4' focal length and f/D = .442. The reflecting surface consists of a fine metallic mesh mounted on an aluminum superstructure. The distance between

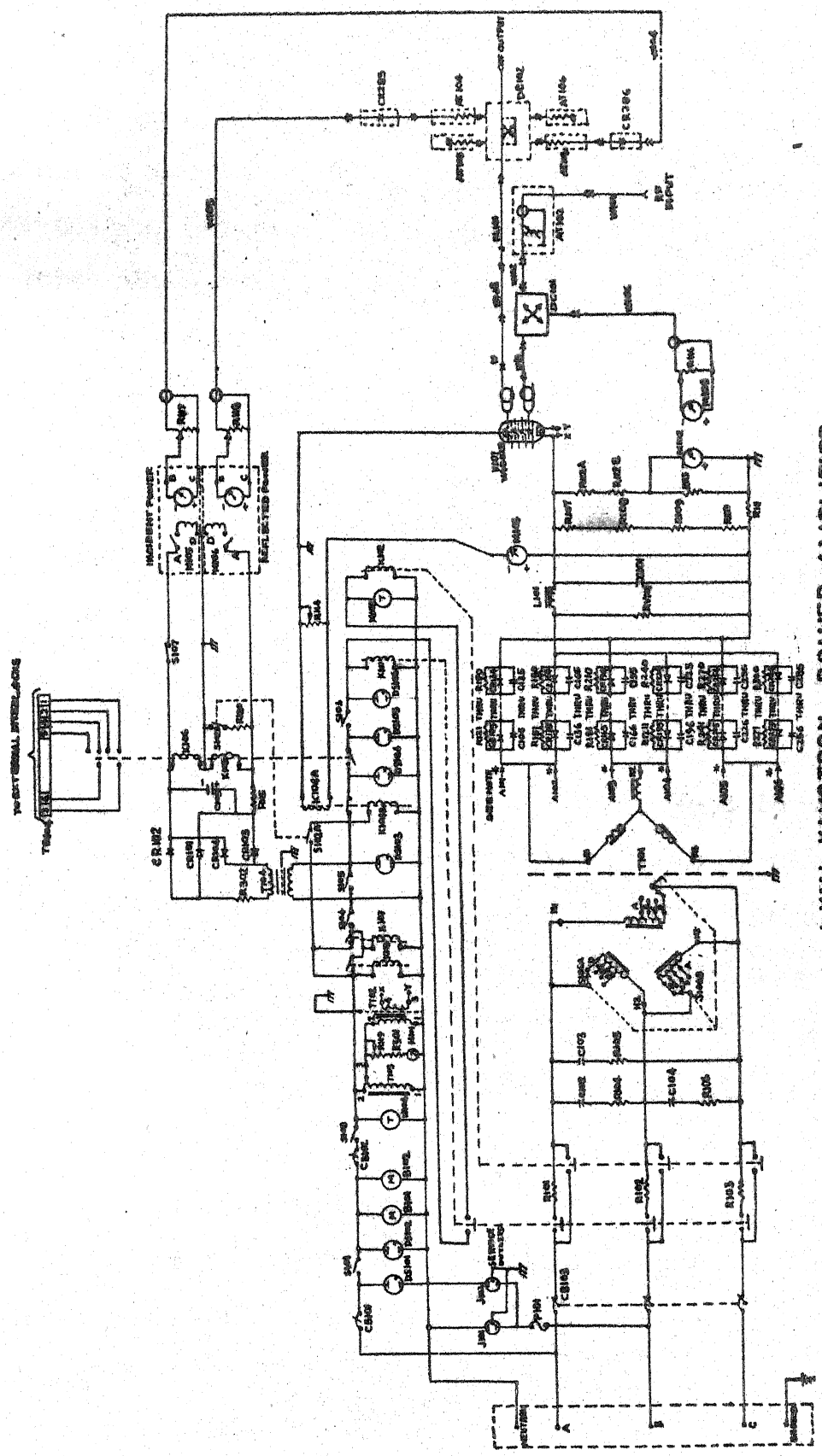

Fig. 2.3: 1 KW. KLYSTRON POWER AMPLIFIER
CIRCUIT SCHEMATIC

transmitting and receiving antennas is 330 Km. The Tx antenna is mounted on a steel structure at U.P. State Observatory, Nainital, almost at ground level, at a height of 6150' above mean sea level. The Rx antenna is mounted on a steel structure 60' high at I.I.T. Kanpur, 415' above mean sea level. The horn feed to the reflector is held in position at the focus by a circular metal ring of 2' diameter. The ring in turn is supported by a tubular tripod support fastened with the peripheral tubular number of the reflector. A side view of Rx antenna system is shown in Fig. 2.4, as it existed prior to the modificatio of foed assembly.

A pyramidal horn serves as primary feed to the reflector. The horn is provided with straight E and H plane flares with TE_{10} wave in the waveguide. The horn is fed by a $1\frac{5}{8}$" high power cable connected through a coaxial to waveguide transition. A sketch of horn feed is given in Fig. 2.5.

2.3.1 Modifications to the Antenna System:

Feed assembly was modified by incorporation of an additional feed horn, lateraly displaced with respect to the main feed horn.

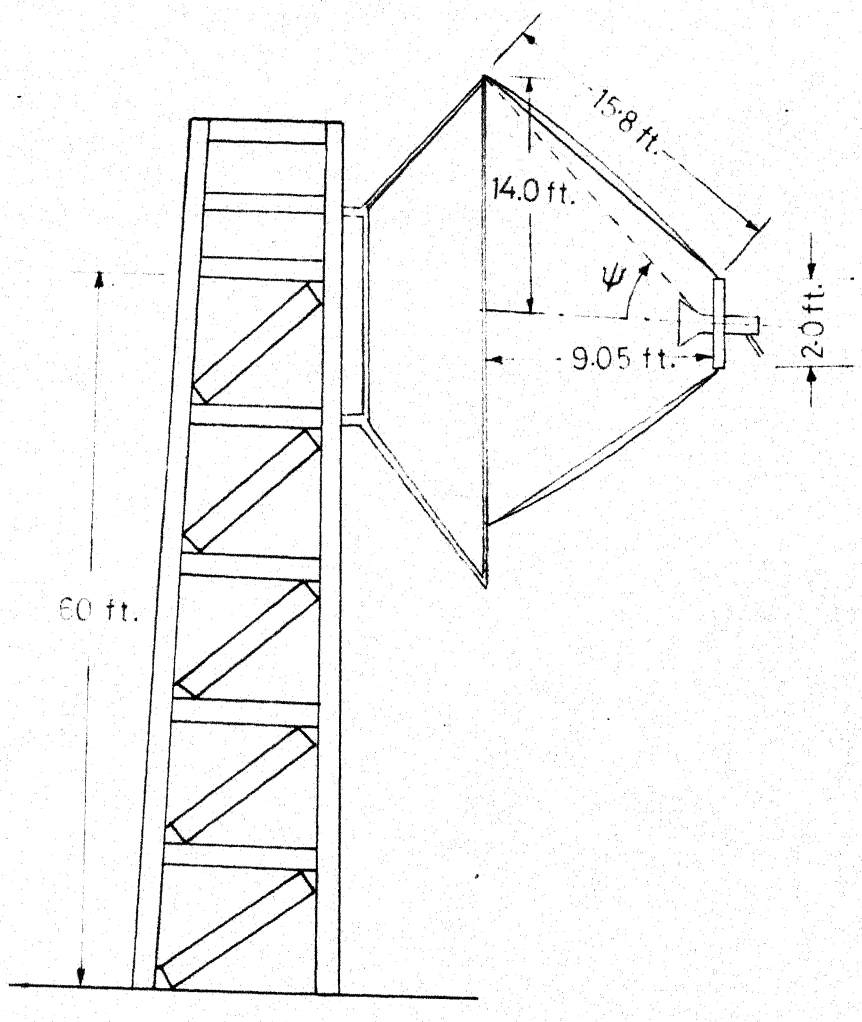

Fig. 2·4 Receiving Antenna System (side view)

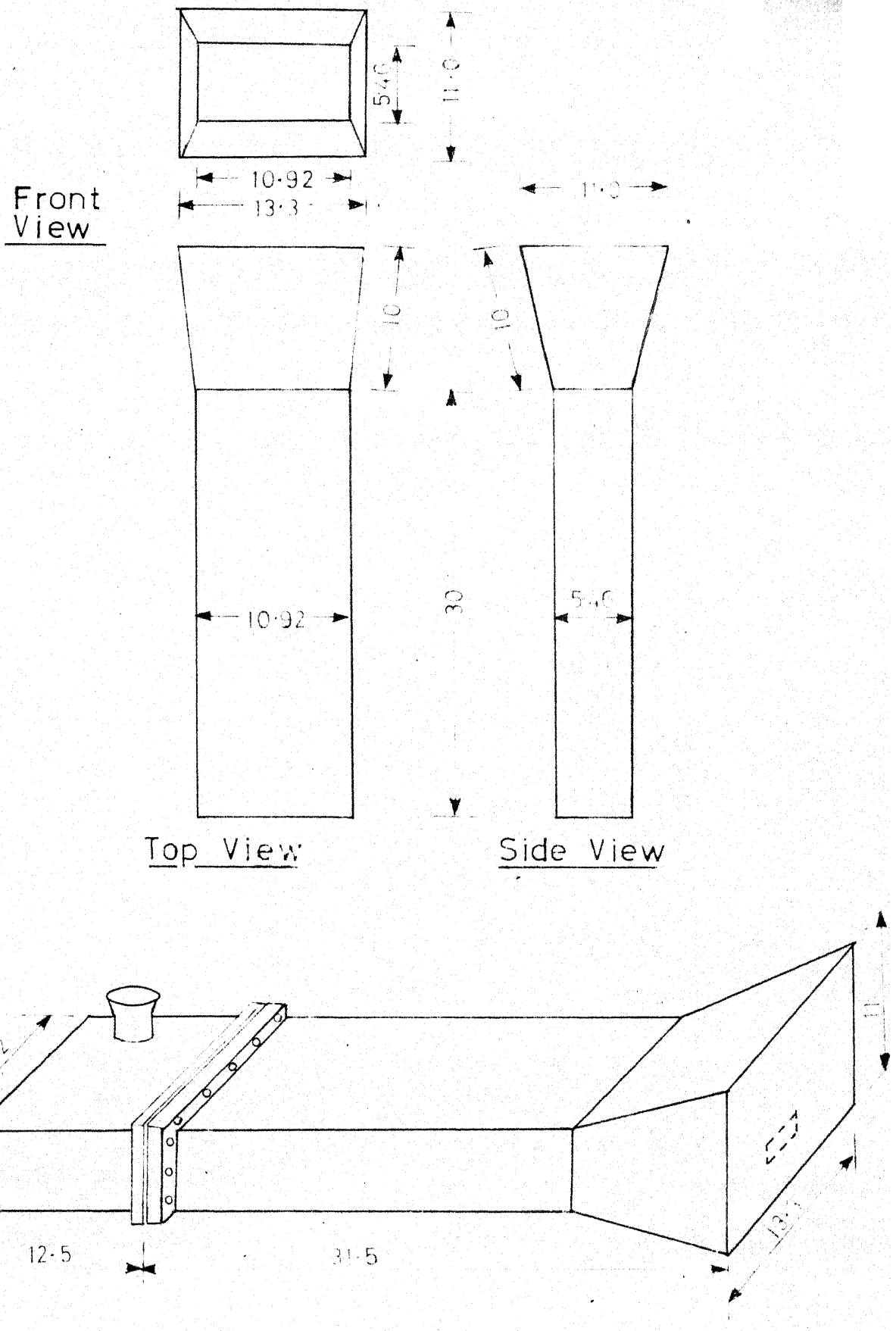

Fig. 2·5 Horn Feed with Waveguide to Coaxial transition

2.3.1.1 Fabrication of Feed Horn:

A pyramidal feed horn having dimensions similar to the existing feed horn was fabricated in the workshop of I.I.T. Design criteria for a pyramidal feed horn is given in Appendix A. Data pertinent to the feed horn is as follows.

E plane aperture - 11.0 cms
H plane aperture - 13.3 cms
Wave guide dimensions - 10.92 cms x 5.46 cms
Length of the horn L - 10 cms
E plane flare angle $\emptyset_E$ - 16.4°
H plane flare angle $\emptyset_H$ - 6.8°

Brass plates of $\frac{1}{8}$" thickness were used for making the waveguide and the horns, while the flanges were made of 3/8" thick brass plates.

The inner surface of waveguide as well as horn was given a fine surface finish by lapping the plates. Assembly was done by soldering, after mounting the plates on a wooden jig of proper dimensions specially made for this purpose. The machining job was done in A.C.E.S. Workshop of I.I.T., soldering in the Central Workshop and lapping of brass plates was arranged from outside sources.

Signals were taken out of the waveguide by means of a waveguide to N type transition. Signals were picked up from the waveguide by means of a probe made of 5 mm thick solid brass rod, which was kept at a distance of $\lambda_g/4$ = (4.72 cms) from the closed end of waveguide. The height of the probe was found to be 3.5 cms for minimum VSWR. To decrease the VSWR further, two tuning screws were used between the probe and the closed end of waveguide adapter, seperated by a distance of $\lambda_g/8$ from each other. By proper adjustment of tuning screws a VSWR of 1.04:1 could be obtained at a frequency of 2.1 GHzs. VSWR was found to be within 1.1:1 for a $\pm$10 MHzs variation of frequency around 2.1 GHzs. Test set up for adjustment of minimum VSWR is given in Figure 2.6.

2.3.1.2 Modification of Feed Assembly:

Effect of feed displacement on the radiation pattern of a parabolic reflector fed with a pyramidal horn has been discussed in Appendix B. It is seen from the radiation patterns, that for a feed displacement of 1 λ, the main beam is shifted by an angle of approx. 1.8°. The second horn was mounted at a distance of 1 λ (14.29 cms) below the main horn.

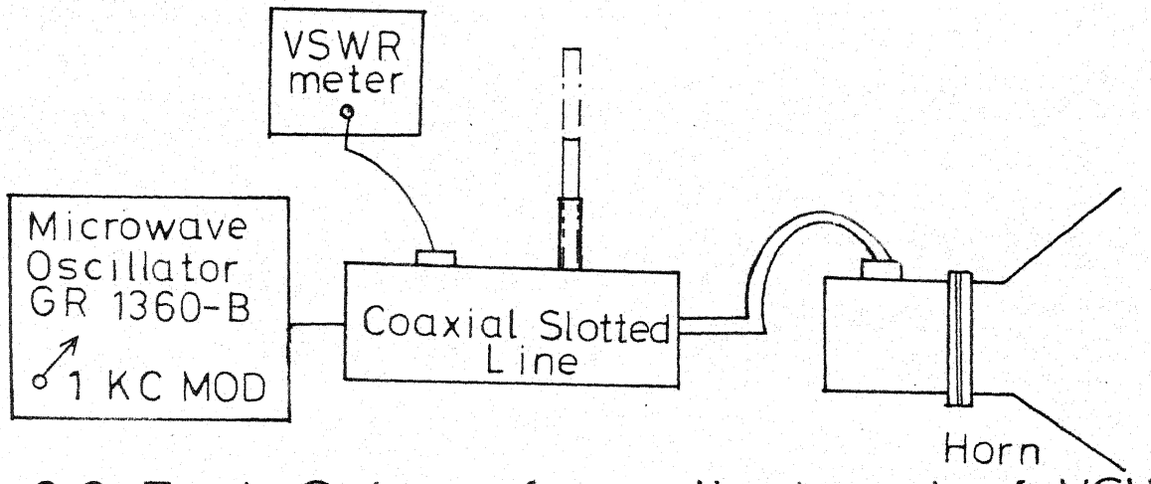

Fig. 2·6 Test Setup for adjustment of VSWR

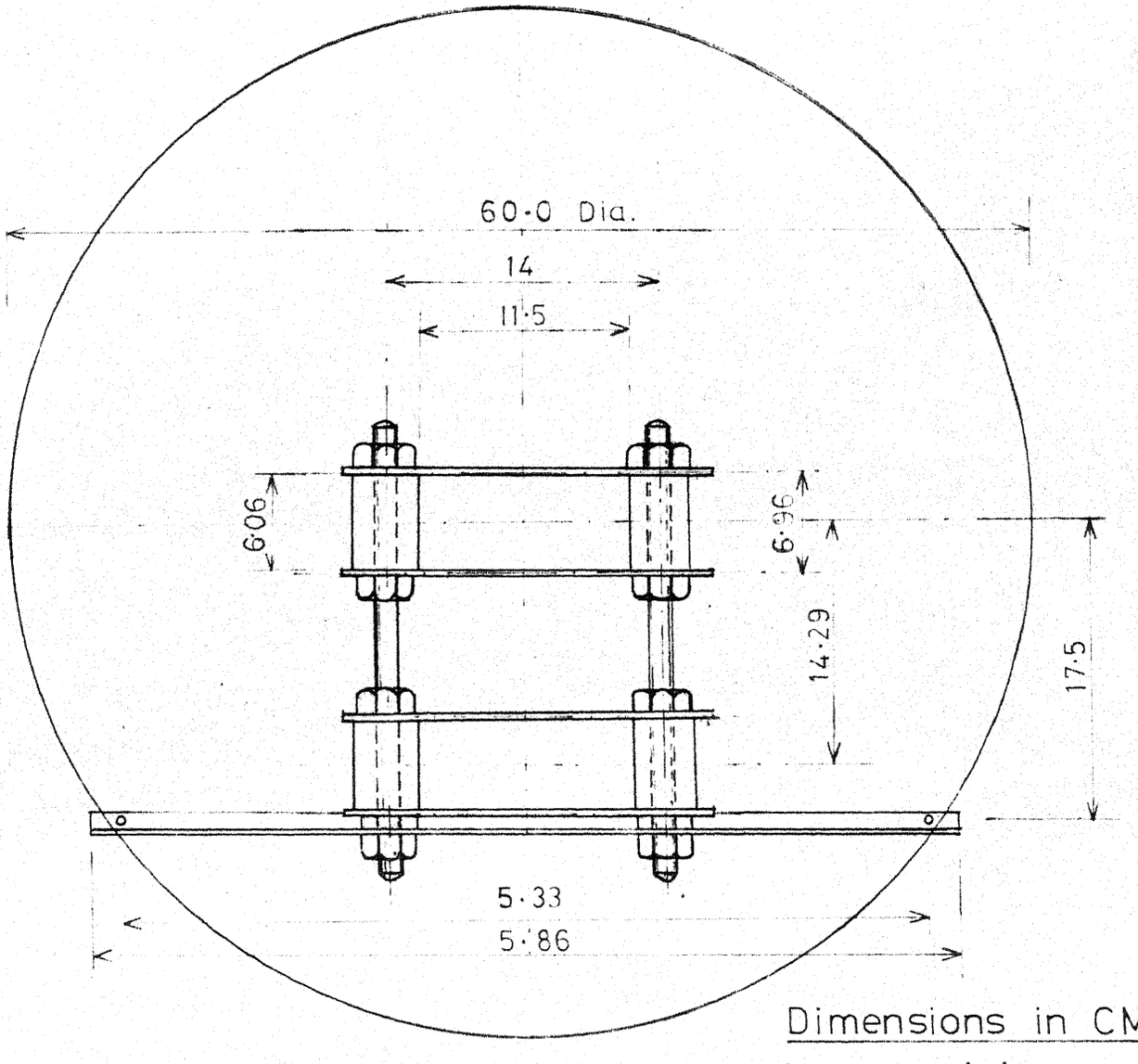

Fig. 2·7 Modified Clamp Assembly

While the circular metal ring of 2' diameter was kept as such, the clamping arrangement was modified to accomodate two horns. A front view of the modified clamp assembly is shown in Figure 2.7.

Since there was no facility for carrying out modifications to the feed assembly at a height of 60' above ground level, a bamboo scaffolding was constructed with a platform of the size 3' by 6' at a height of about 55' so that modifications could be carried out to the feed assembly.

The RG-9 A/U coaxial cable that was available for bringing the signal from the second horn to the receiver input was found to have a loss of 13.5 db. The new feed horn with this high loss cable was therefore kept in the middle position, while the original feed horn with the $1\frac{5}{8}$" connector and low loss cable was kept in the displaced position. The expected difference in the signals received by the two horns due to the differences in path losses was thus partially compensated by the difference of feeder losses between the horns and receiver input (Details of calculations for path loss are given in Appendix C).

2.4 Receiving System:

The receiving system consists of two main parts

i) 2.1 GHzs receiver
ii) Signal conditioning unit

2.4.1 2.1 GHzs Receiver:

This is a double superheterodyne receiver using a coherent delection scheme. The coherent reference signal is generated within the receiver by using a tracking PLL having a narrow loop bandwidth. Block schematic of the receiver is given in Fig. 2.8.

R.F. input from antenna is fed to the signal port of a double balanced mixer, while a 2.17 GHzs signal generated by passing a 54.25 MHzs crystal oscillator output through a buffer amplifier, a doubler-doubler and a S.R.D. multiplier, is fed to the local oscillator port of the balanced mixer through a variable attenuator.

70 MHzs output from the mixer is amplified by a preamplifier with a gain of 40 db and a bandwidth of 800 KHzs centred around 70 MHzs. This is followed by a main amplifier with variable gain up to maximum of 40 db. The mixer-2 and IF-2 amplifiers are built in the same unit, which has also a built in frequency synthesizer, which generates a frequency of 65.1 MHzs by mixing the xtal frequency of 54.25 MHzs with a frequency of 10.85 MHzs, generated by dividing the xtal frequency by 5. This 65.1 MHzs frequency, when mixed with the 70 MHzs IF 1 frequency, gives a nominal IF 2 frequency of 4.9 MHzs.

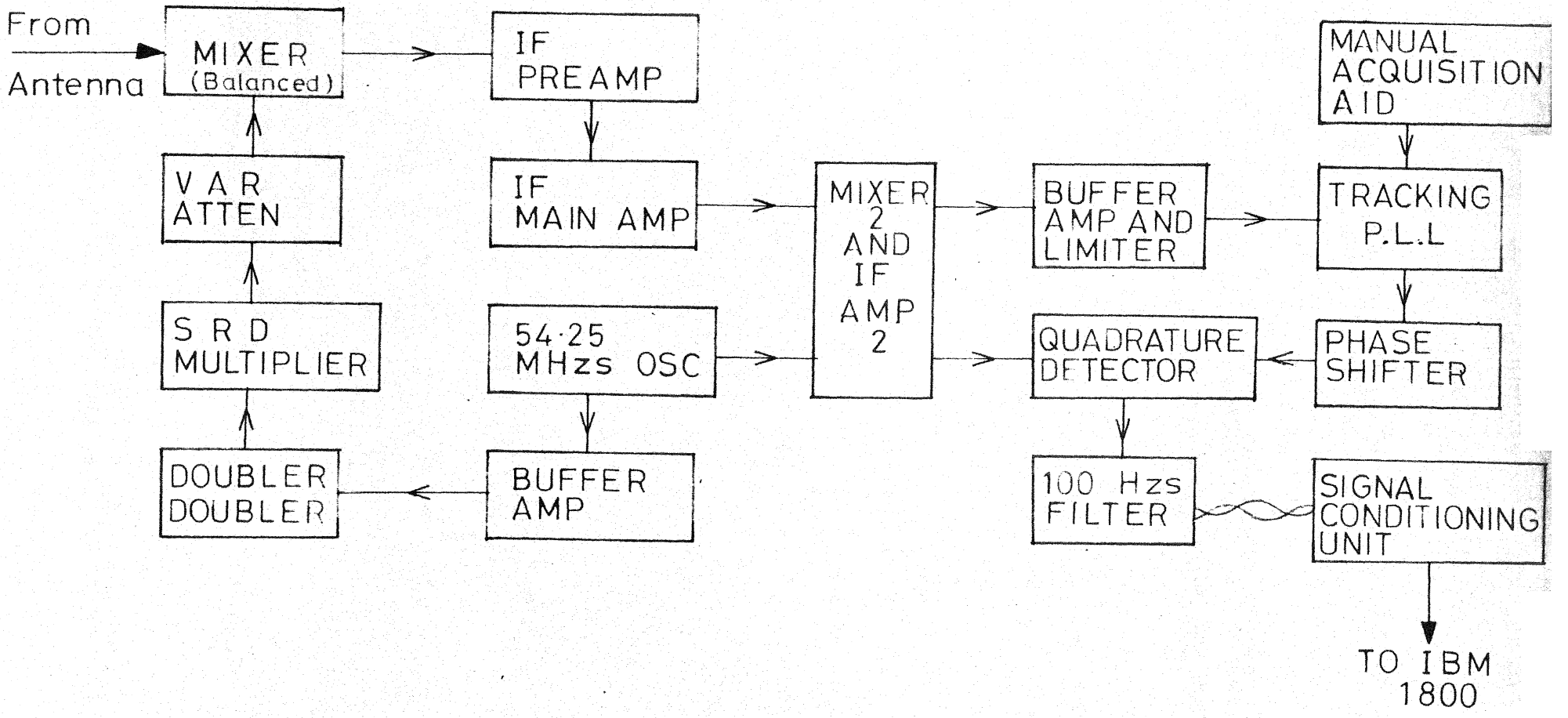

Fig. 2·8 Block Diagram 2·1 GHzs Receiver

Output of mixer 2 is fed after limiting, to a phase locked loop having a bandwidth of 160 Hzs. The limiter gives the loop an adaptive behaviour, as the signal level at the output of mixer 2 changes, depending on the strength of 2.1 GHzs received signal.

The VCO frequency is further phase shifted by 90° before applying to the input of a quadrature detector. IF 2 output is connected to the other input of this quadrature detector. Output of detector is a d.c. voltage whose amplitude varies linearly in proportion to the incoming signal, as the signal varies from receiver threshold upto the saturation level of -65 dbm. The output of quadrature detector is passed through a 100 Hzs low pass filter, before it is carried to IBM 1800 room by a long insulated shielded twisted pair of wires.

The tracking PLL is built by using a single XR-S200 IC chip and the product detector uses the analog multiplier and operation amplifier sections of another XR-S200 chip 100 Hzs low pass filter is of the sixth order Butterworth type with -3 db cut off frequency of 100 Hzs and having a built-in d.c. offset adjustment control in the form of a panel mounted ten-turn helipot.

2.4.1.1 Modifications to the Receiver:

A coaxial r.f. switch was introduced before the balanced mixer. The switch HP8761A has a switching speed better than 50 ms, insertion loss < 0.5 db between DC-12 GHzs and a isolation of > 50 db. The switch was operated by means of a bipolar switching pulse of ± 15V generated by the Data Interface Unit.

The gain of the main IF amplifier was increased to 55 db from the original value of 40 db. This was necessary as the median signal levels at the receiver input were likely to be about 15 db lower than in the original system.

Necessary control pulses for the synchronised operation of r.f. coaxial switch and the process I/O unit of IBM 1800 were generated by means of a data logging interface designed specifically for this purpose. The details of data logging interface are given in Section 3.3.

2.4.2 Signal Conditioning Unit:

The analog signals connected to the multiplexer terminals of IBM 1800 should have proper frequency response, source impedance and dynamic range. This is achieved by connecting the signal through proper low pass filters and amplifiers. Output of 100 Hzs filter is

brought to IBM 1800 room through an insulated shielded twisted pair ofwires and is applied to the input of a high CMRR guarded input amplifier. For recording slow fades, output of the amplifier was connected to a 10 Hzs filter having a slope of at least 20 db/octave above the cut off frequency. The output of this filter was connected to relay multiplexer input of IBM 1800.

2.4.2.1 Modifications to Signal Conditioning Unit:

The d.c. voltage at the output of modified receiver was switched between two different levels which could vary anywhere between a few miltivolts to 3 volts as the receiver was switched between two horns. It was observed that the time constant of the 10 Hzs filter (15 msec) was not sufficient for the D.C. levels at the input to the multiplexer to change to their new values, between the time the switching took place and the time at which the sampling of analog input commenced (25 ms). This filter was therefore taken out of cct. 100 Hzs filter was retained in the cct, to obtain the desired gain, since the time constant of this filter was quite small compared to 25 ms. The output was fed to solid state multiplexer input, instead of relay multiplexer input, since the max. repetition rate per point for Relay multiplexer was 50 samples/sec.

2.4.3 Caliberation of Receiving System:

The receiving system was given an initial warm up of 3 to 4 hours. The D.C. offset controls in the 100 Hzs filter in the receiver as well as the amplifier in the signal conditioning unit were adjusted so that the D.C. voltage at the solid state multiplexer input was as close to zero as possible in the absence of any input. A 2.1 GHzs signal from r.f. signal generator HP type 8614A was now fed to one of the input ports of r.f. switch and the IF stages were tuned for max. gain. The D.C. output at the solid state multiplexer input was now recorded for different r.f. inputs, after adjusting the PLL V.C.O. manual frequency control for the best lock. With the available signal generator proper locking could not be done for signal levels below -100 dbm.

CHAPTER 3

DATA LOGGING SYSTEM

3.1 Choice of Data Logging System:

It was desired to have a data-logging system capable of truly reproducing the slow variations in the signal level due to fading, as well as the abrupt variations in the signal level when the receiver was switched between two horns. In addition there was a need to store the data to facilitate any further analysis. The obvious choice was the use of real time computer IBM 1800 having a disk storage as well as tape storage facility and a facility for conversion of analog input signals to digital values by a built-in A.D. converter.

3.2 Salient Features of IBM 1800:

This is a real time computer also called a process computer having three additional facilities compared to a general purpose computer.

i) Interrupt facility
ii) Process Input-output devices
iii) Real time clocks

The interrupt facility gives the computer, power to suspend the execution of a current program and save it for execution at a later time, in order to execute another higher priority program.

The process input-output devices are used to send/receive signals to/from the computer. This facility enables the computer to handle electrical signals directly for processing. It accepts both analog and digital signals.

The real time clock is used to collect data at a specified time. Configuration of IBM 1800 data acquisition and control system is shown in Fig. 3.1a. In our experiment we have used the process I/O facility. This is divided into four general categories

i) Analog input
ii) Digital input
iii) Analog output
iv) Digital output

The analog input feature which has been utilised consists of an analog to digital converter, a comparator and two types of analog input multiplexers.

The characteristics of A.D.C. are as follows:

Input type	- voltage, bipolar
Input level	- 0 to $\pm$ 5 volts
Input impedance	- 10 Megohms or greater
Output value	- 8, 11 or 14 bits plus sign
Conversion time	- 29,36 or 44 micro seconds
A.D.C. rate	- 9K, 10K, or 11K conversion per second.

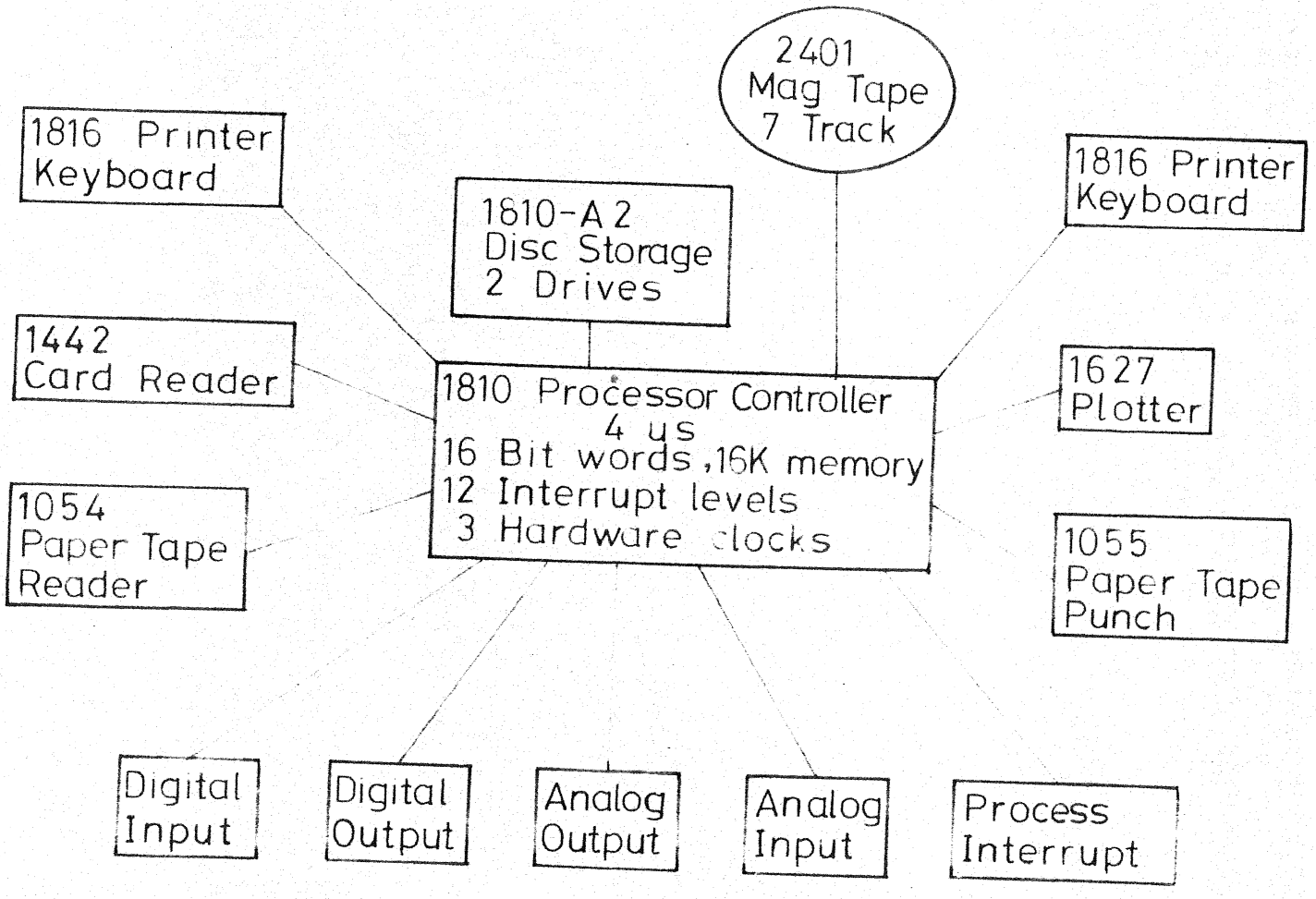

Fig. 3·1 IBM 1800 Data Acquisition and Control System Configuration

The comparator performs automatic range checking on digital values developed by ADC.

Multiplexer-R unit provides relay multiplexing of 100 points per second with high input resistance. It consists of a group of 16 points for multiplexing of low or high level (-0.5 to +5 volts) differential analog input signals with high common mode voltage operation (200 volts) and high common mode rejection. Maximum repetition rate per point is 50 samples/sec.

Multiplexer-S unit provides solid state high speed multiplexing (10 KHzs max. with 11 bit resolution with Mod 1 ADC) of high level signal ended analog input signals.

Conversions can be synchronised from an external signal. It is this external synchronisation facility that has been used in the design of data logging interface described in the next section.

3.3 Data Logging Interface:

The data logging interface was developed to synchronise the operation of r.f. coaxial switch and the process I/O unit of IBM 1800.

Block schematic of the interface is given in Fig. 3.2. It consists of two main units

i) Computer Interface Unit
ii) Switch Control Unit

After the solid state multiplexer input point to be sampled is addressed by the computer, a 'Ready' signal is transmitted by the computer to the computer interface unit. Ready signal specifications are as given below:

Down level - -12V through a 1000 Ω resistor

Up level - 0.0V to -0.5 volts

The positive going transition of 'Ready signal' triggers a monostable after suitable level translation, which generates a 25 ms wide TTL level pulse. The tracking edge of this pulse generates a 4 μs wide 'sync. pulse', which is fed back to IBM 1800. A 50 ms wide control pulse is sent to the switch driver through a peripheral driver, 200 ft. long twisted balanced pair and a balanced receiver. The switch driver generates a bipolar switching pulse for operation of r.f. coaxial switch.

On receipt of the 'Sync. pulse', the process I/O unit completes the action of analog to digital conversion of the signal, at the solid state input point that has been addressed, and brings the 'Ready' signal down. The analog

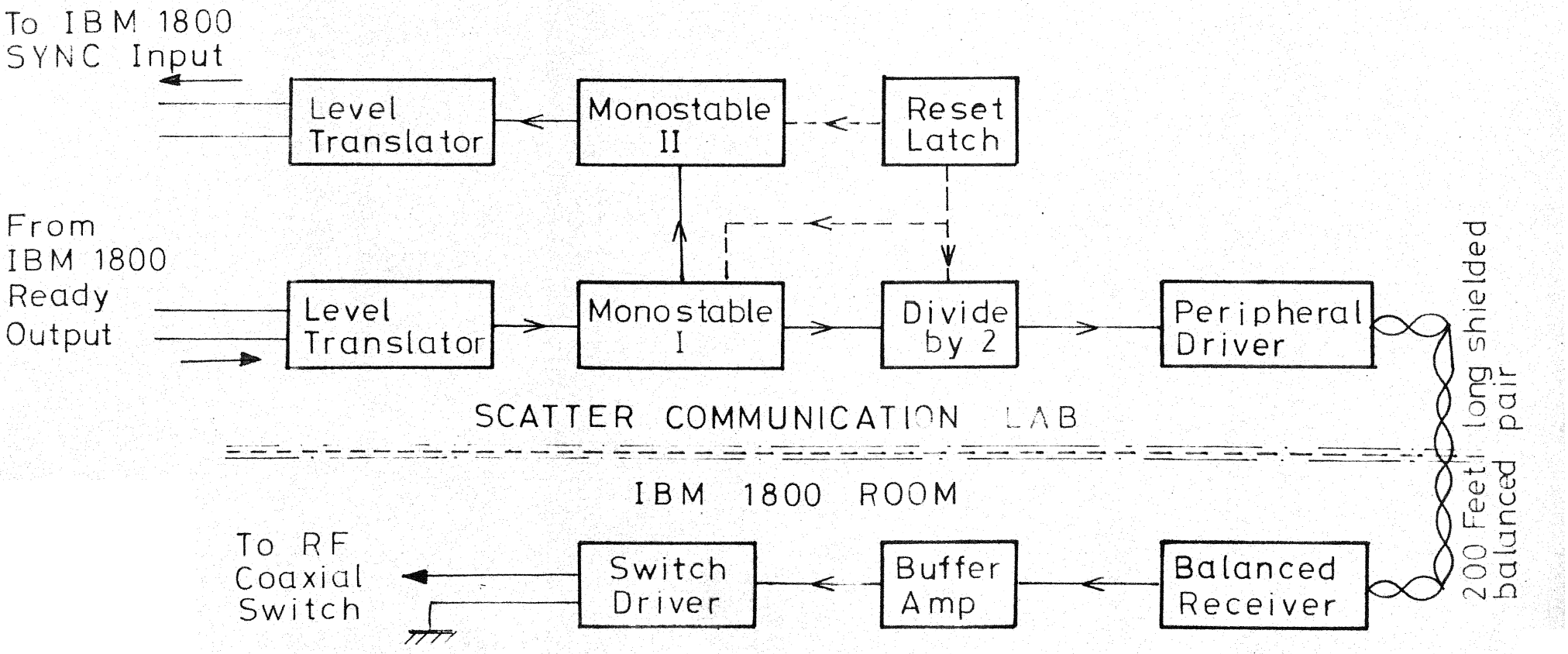

Fig. 3·2 Block Schematic Data Interface Unit

input point is addressed again after a program controlled delay and the cycle is repeated. The width of control pulse and the position of 'sync.' pulse are adjustable by means of a front panel control. The timing diagram of the data interface is given in Fig. 3.3.

Detailed cct description of computer interface unit and RF switch control unit are given below.

3.3.1. Computer Interface Unit:

A schematic cct of computer interface unit is given in Fig. 3.4 and the P.C.B.lay out is is given in Fig. 3.5.

The positive going transition (Fig. 3.3a) of 'Ready' pulse causes the transistor Q, to become conducting , so that its output goes from a high state to a low state (Fig. 3.3b). Output of Q, is connected to one gate of the quadr-2 input Nand gate 7400 (I1), connected as an inverter. Therefore at the output of this stage we get a transition going from a low level to a high level (Fig. 3.3c).

This positive going TTL level transition causes a monostable ($\frac{1}{2}$ of 74123) to trigger and generate a pulse of width 25 ms (Fig. 3.3d). Pulse width is decided by capacitor C_{ext} and resistance R_6 according to the relation

$$T_{\omega} = 0.32\, R_6\, C_{ext} \left(1 + \frac{0.7}{R_6} \right)$$

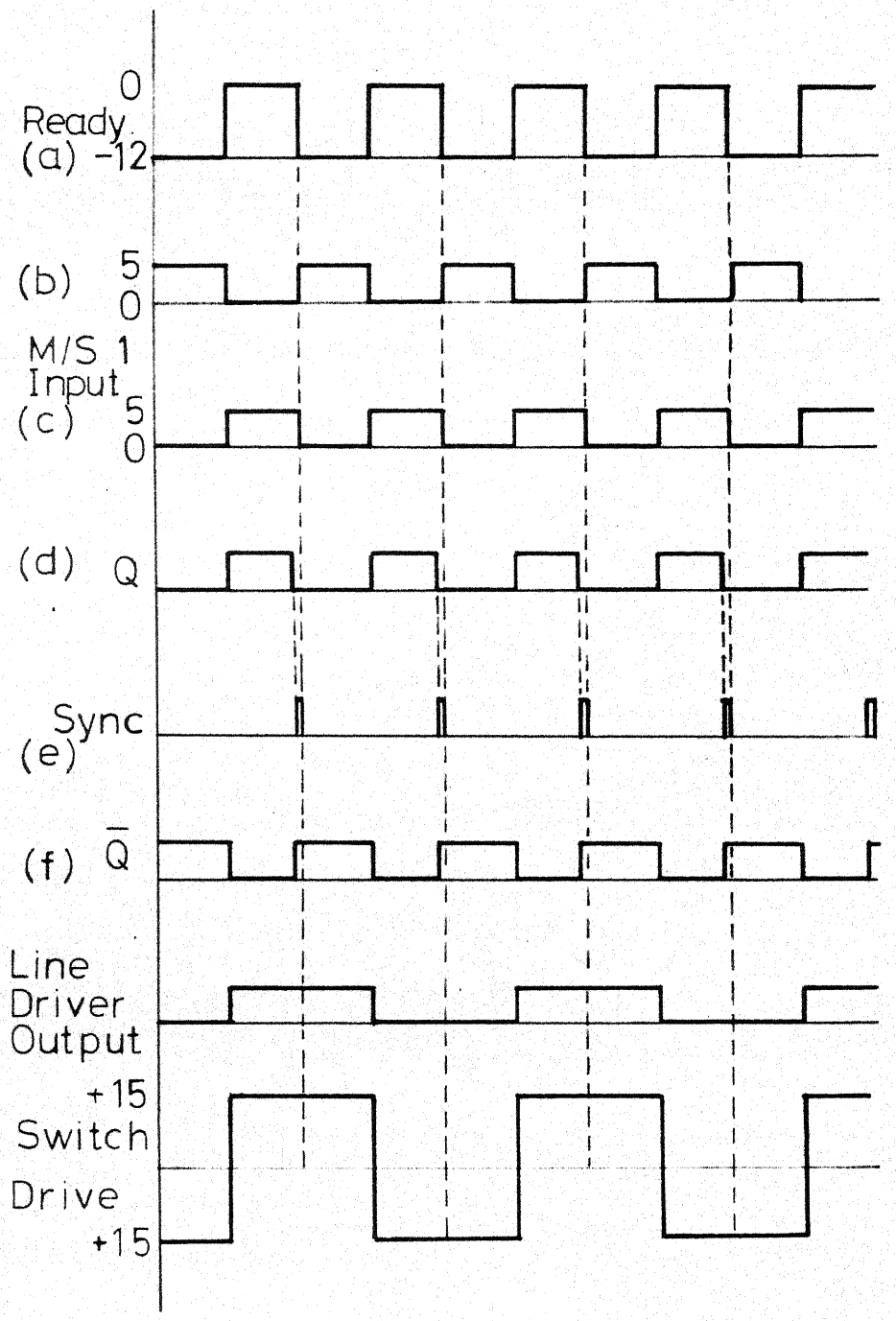

Fig. 3·3 Timing Diagram Data Interface Unit

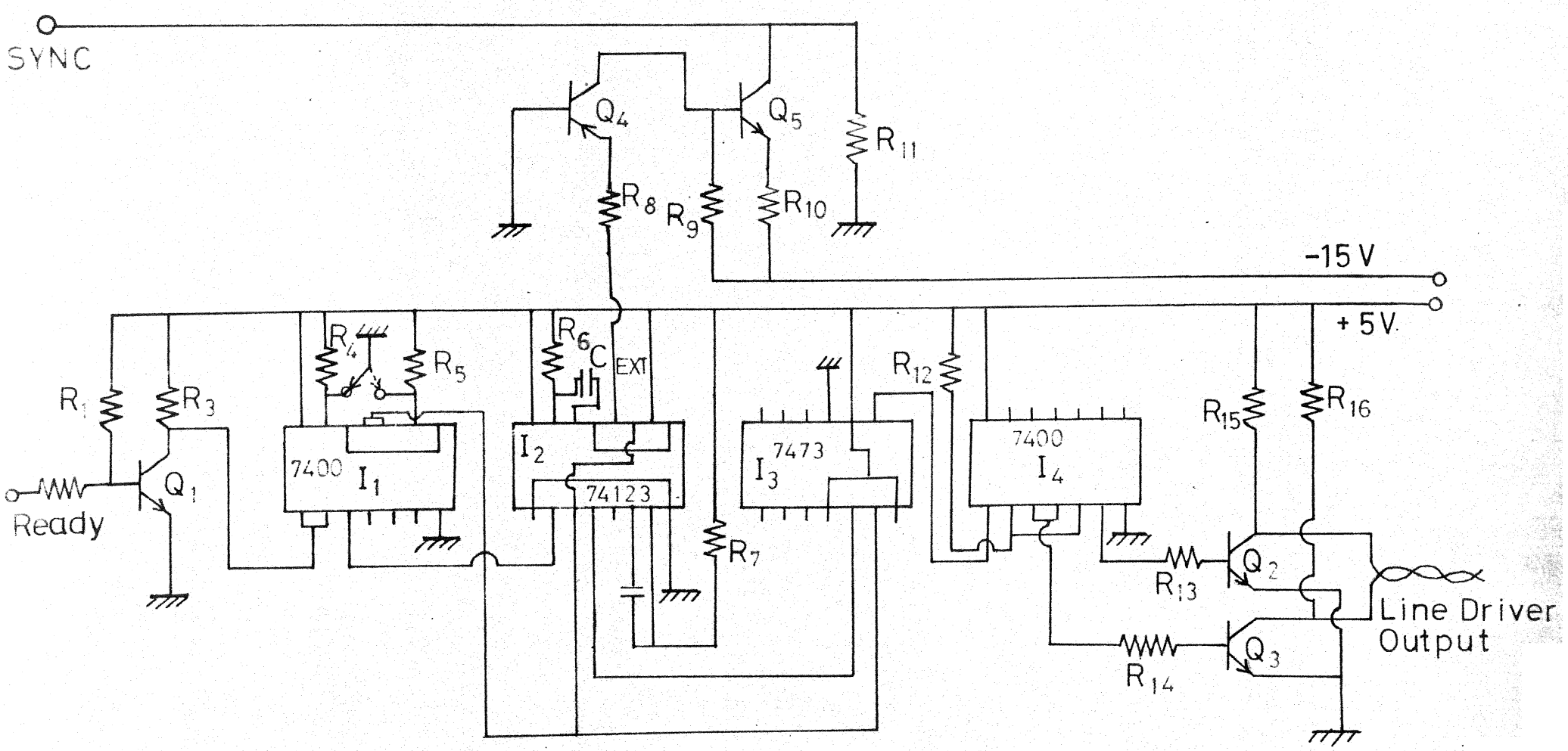

Fig. 3·4 Cct Schematic Computer Interface Unit

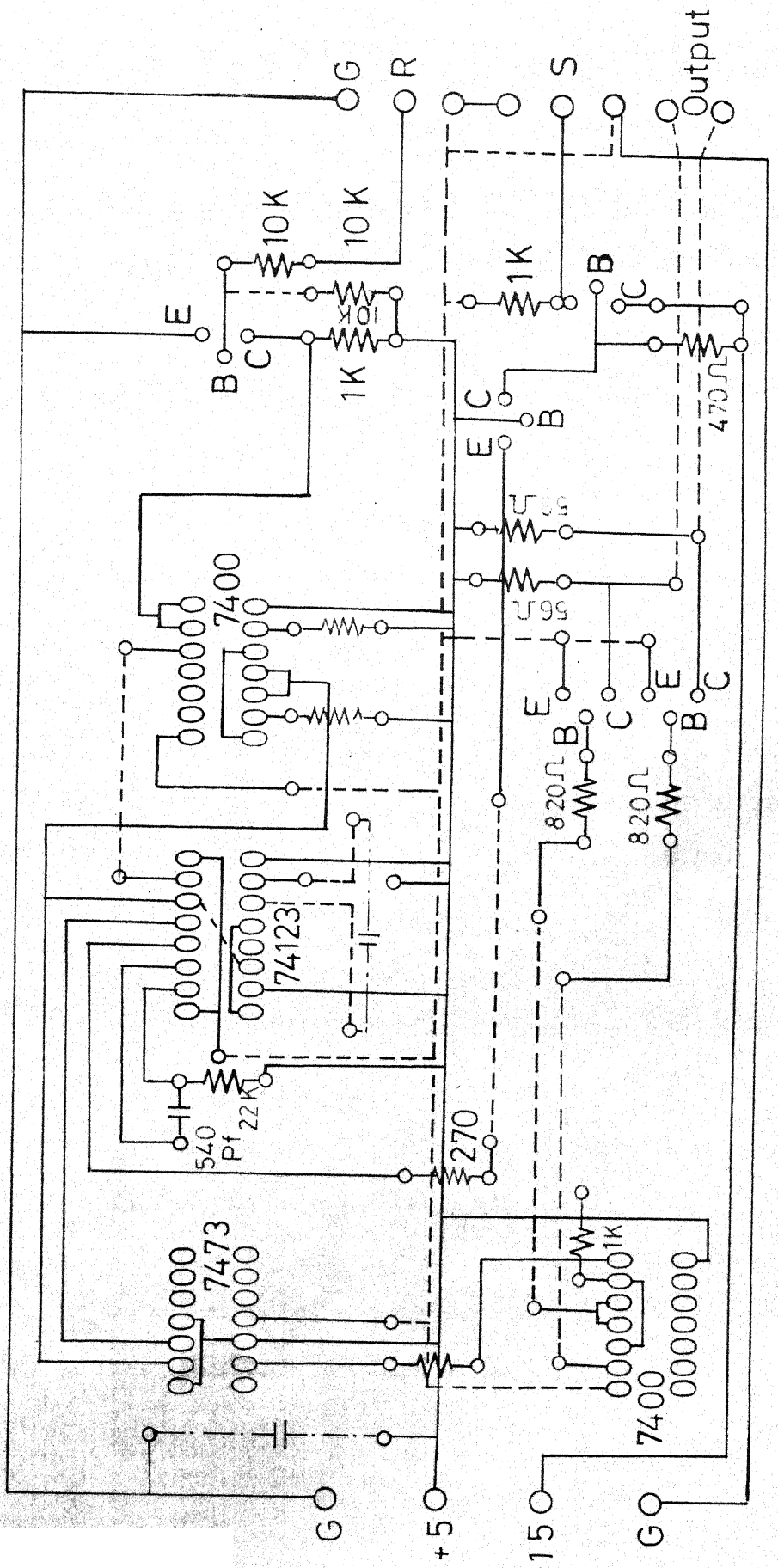

Fig. 3.5 PCB Layout Computer Interface Unit

Truth table of monostable is given in Fig. 3.6. The $\bar{Q}$ output of monostable 1 triggers the monostable 2 during its trailing edge since the B_2 input is kept permanently high. Monostable 2 (2nd half of 74123) produces a 4μs wide TTL level pulse which is delayed by 25 ms with respect to ready pulse. The $\bar{\theta}$ output of monostable 2 is connected to the emitter of PNP transistor 2N404 connected in common base configuration. The collector of 2N404 is connected to the base of 2N2369 transistor. When the $\bar{\theta}$ output goes from high to low level for a period of 4μs, transistors 2N404 and 2N2369 become non-conducting and the collector of 2N2369 goes from -15V to 0 V for this period giving a 'sync' pulse, which is fed back to IBM 1800, and causes 'Ready' pulse to go down. Ready pulse goes up to 0 V again after a program controlled delay of 25 ms.

The $\bar{Q}$ output of monostable 1 is passed through a dual J-K M/s Flip-flop, which is triggered at every negative going transition, thus giving a 50 ms wide pulse at the output of the divider cct (see timing diagram). Two gates of 7400 (IC-1) are wired as a latch to provide clear pulses to 74123 and 7473. This helps in resetting the r.f. switch to one position in the beginning of the experiment.

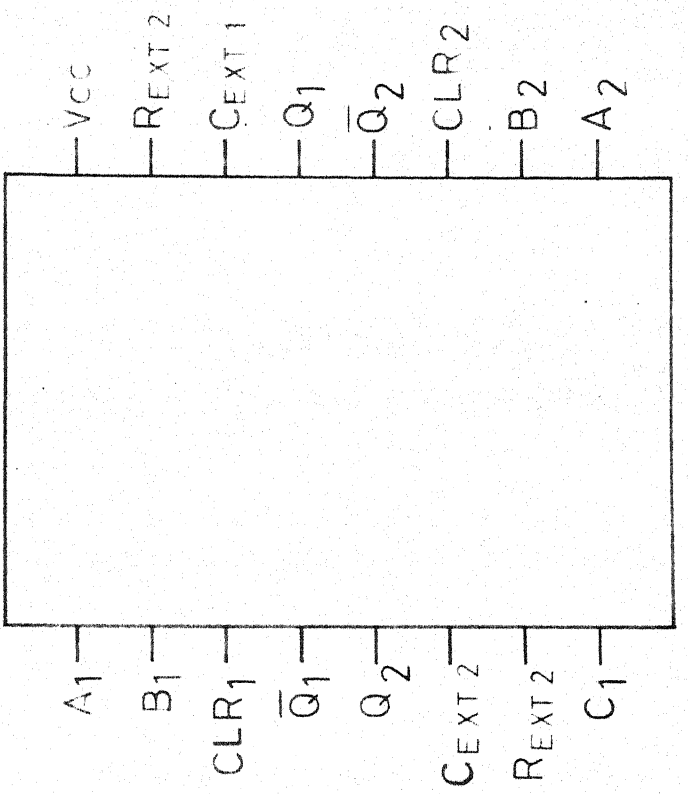

Fig. 3·6 a Pin Connection 74123

Inputs			Q	Q̄
A	B	CLR		
H	X	H	L	H
X	L	H	L	H
L	↑	H	⌐	⌐
↓	H	H	⌐	⌐
X	X	L	L	H

Fig.3·6 b Truth Table 74123

Since the 7473 output is not capable of driving the 200 ft. length of cable from IBM 1800 DACS centre to the scatter communication room, a balanced line differential driver has been used, which is capable of driving low impedance transmission lines in rather severe noise environments. The balanced driver is provided by nand gate 7400 connected as an inverter. The cct is connected as a collector output balanced driver. The 56 Ω terminations at the driver end of line provide short cct protection for the lines as well as proper termination.

3.3.2 Switch Control Unit (Figs, 3.7 and 3.8):

The line driver output voltage pulse from the computer interface unit is conveyed to the scatter communication room through a twisted pair line, to derive maximum benefit from the driver's capability. The typical impedance of twisted pair is 100 Ω.

The first stage of switch interface unit is a μA 710 comparator, which has got a TTL compatible output. The differential receiver configuration allows a large common mode noise rejection capability. The output of this stage is a TTL level square wave of 50 ms width.

The second stage consisting of op-amp 741 converts this square wave to a bipolar square wave of amplitude $\pm$ 15V and

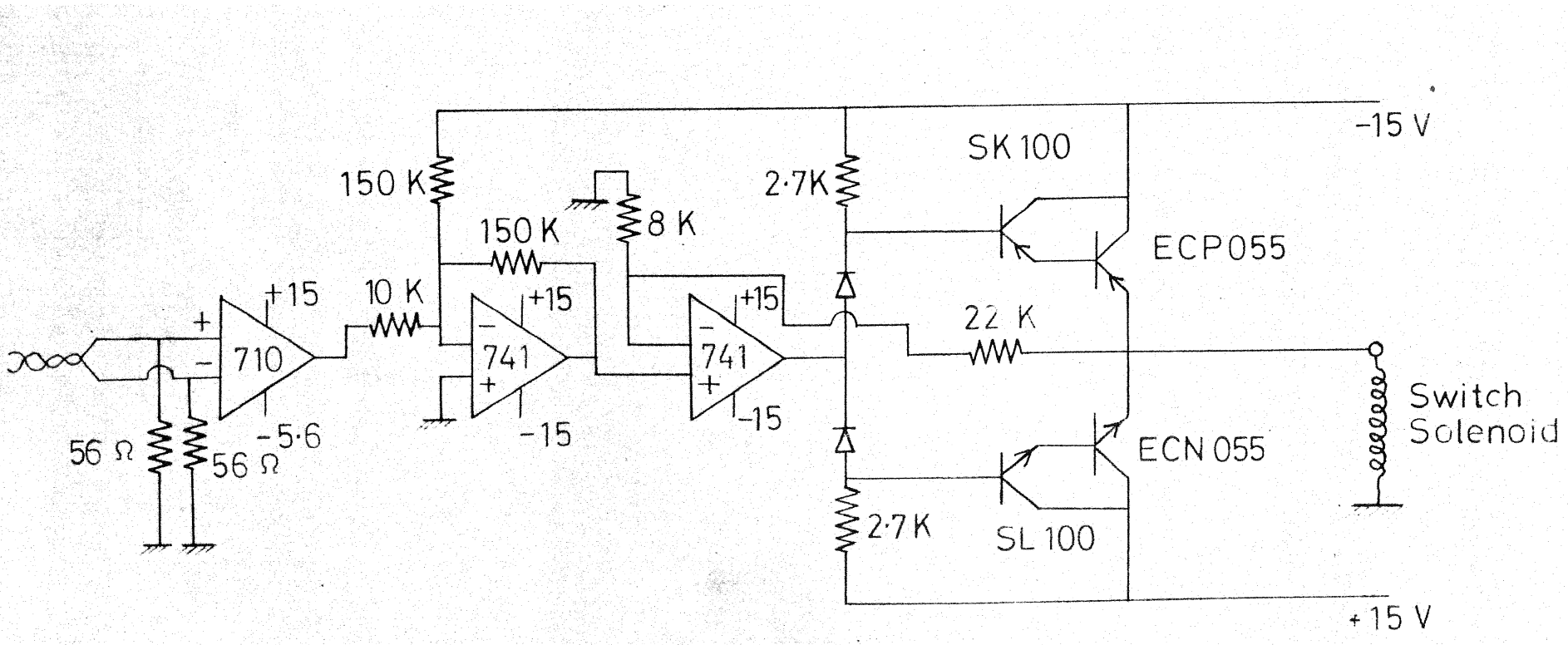

Fig. 3·7 Cct Schematic Switch Control Unit

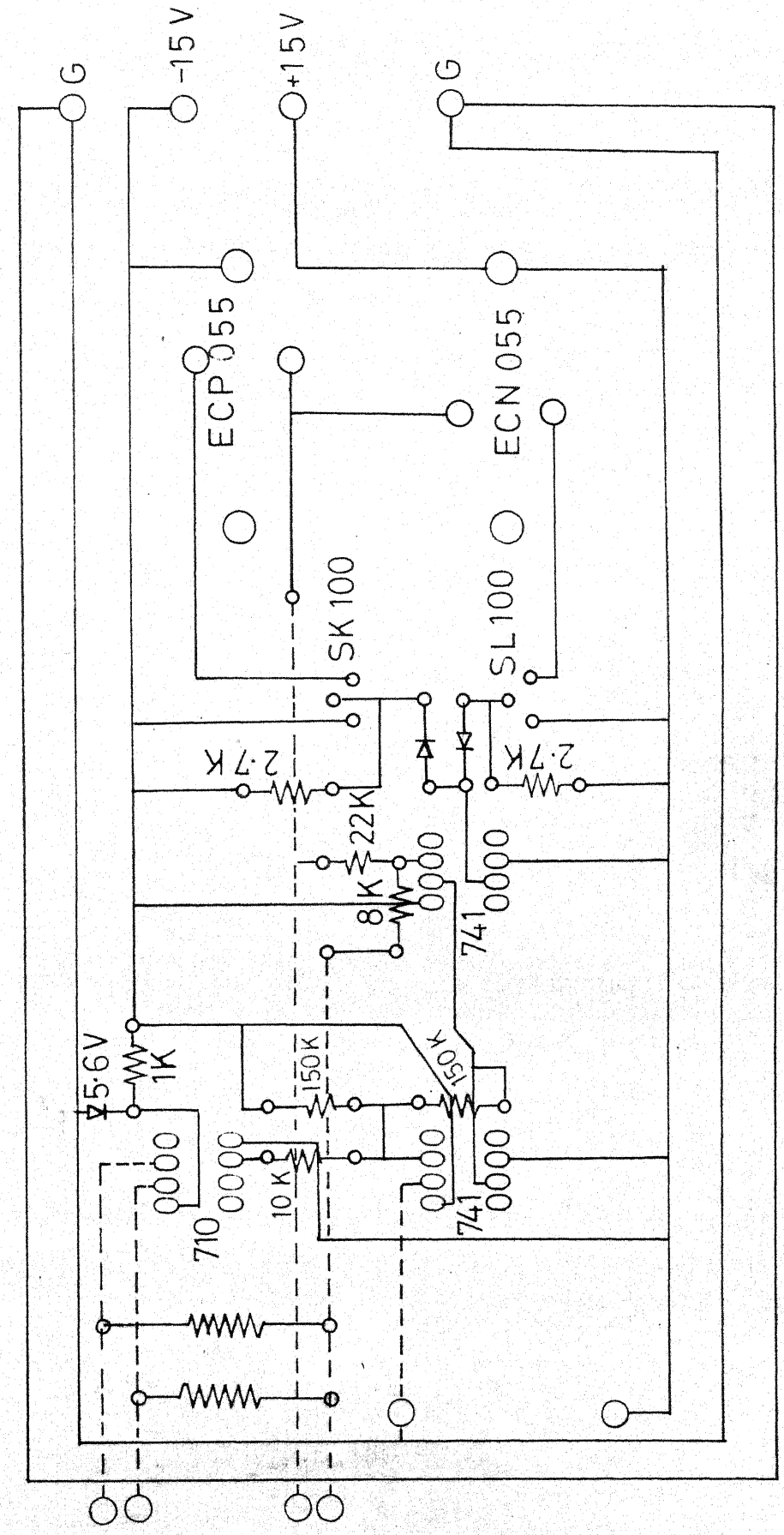

Fig. 3.8 PCB Layout Switch Control Unit

width 50 ms. This is again followed by a 741 in the noninverting configuration, which provides a buffer action and also provides the driving current for the final stage consisting of two Darlington pairs (SK 100 and ECP055) and (SL 100 and ECN055) connected in push-pull, that provide the necessary switching current to the r.f. coaxial switch. The typical current drawn by the r.f. switch, during each switching period is about 100 mA.

3.4 Data Logging Scheme:

Results of many investigators have indicated that a one minute sampling period gives an almost perfect Rayleigh distribution. It was therefore decided to carry out sampling of data over one minute periods. Taking into account the limitations of the switching speed of r.f. coaxial switch, as well as the fading rate considerations, 600 samples from each horn were taken, during this one minute interval. These samples were stored in two different arrays in the digital form and were immediately transferred to a magnetic tape. Each set of data was preceded by a four word header containing time, date, month and set no. of record and succeeded by a four word trailer containing the same details.

A flow chart of programme DATLG developed to carry out the data logging operation is shown in Fig. 3.9. Two options were provided depending on the availability of assistance during data-logging operation. The first option, which was adopted whenever there was some assistance available, was to monitor each set of samples and to transfer only those sets to tape, where the median signal strength observed in both horns appeared to be well above the receiver threshold. The second option was to record a number of sets continuously, the data being automatically transferred to tape at the end of each set. Both options have been utilised.

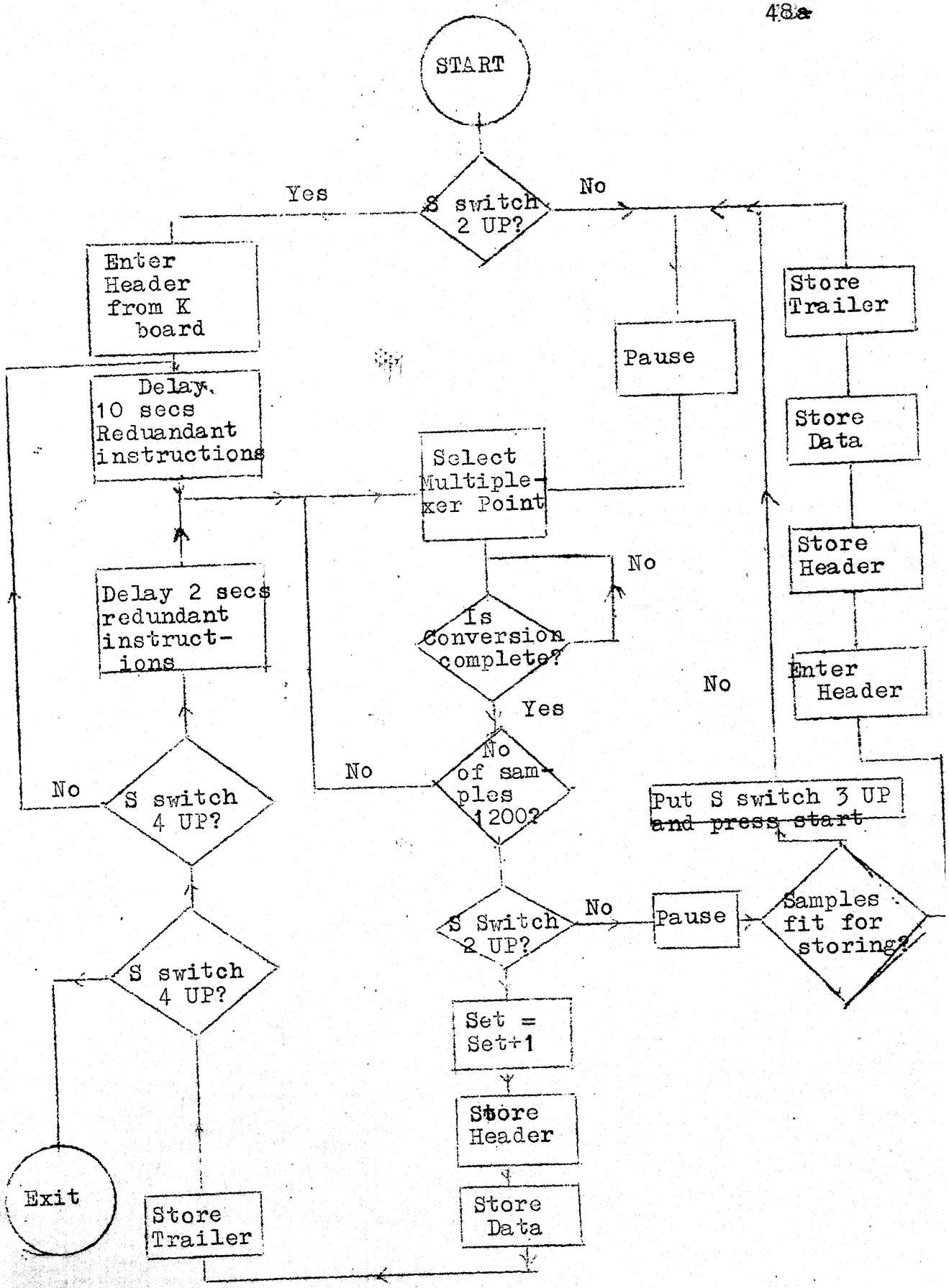

Fig - 3.9

FLOW CHART OF PROGRAM 'DATLG'

CHAPTER 4

DATA ANALYSIS

4.1 Data recorded over a period of one week for different periods of time was analysed to find out the median received signal and sample depth of fade for signals received from each horn, and the correlation coefficient between the samples taken over a one minute period.

By caliberation of the receiving system, it was established that the input to the receiver mixer in db was related to the voltage applied to solid state multiplexer input terminals of the computer by the relationship.

$$(V_{in})db = 20 \log V_{out} - 88$$

where V_{out} is the voltage applied to the solid state multiplexer input terminals in volts.

Programme "BPLOT" given in Appendix D was utilised to obtain plots of Receiver input vs. time for signals from each horn. These plots aid visual presentation of the signal variations with time and the fading characteristics of signals. Some such typical plots are given in Fig. 4.1, 4.2.

Plots were drawn for all the observations taken. After examining the plots, those observations where signal strengths were so weak that their accuracy was not reliable

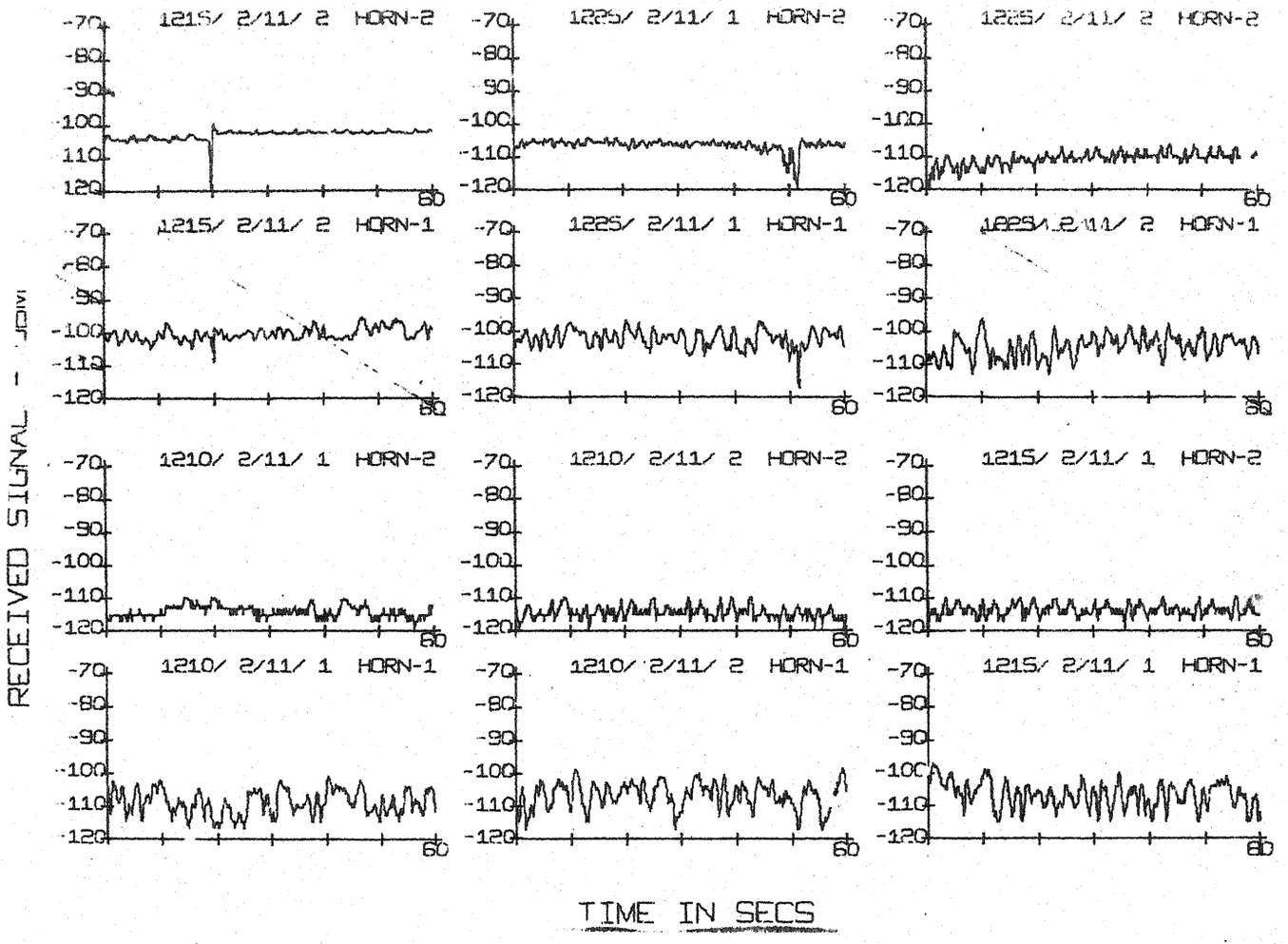

Fig. 4·1 Afternoon Signal

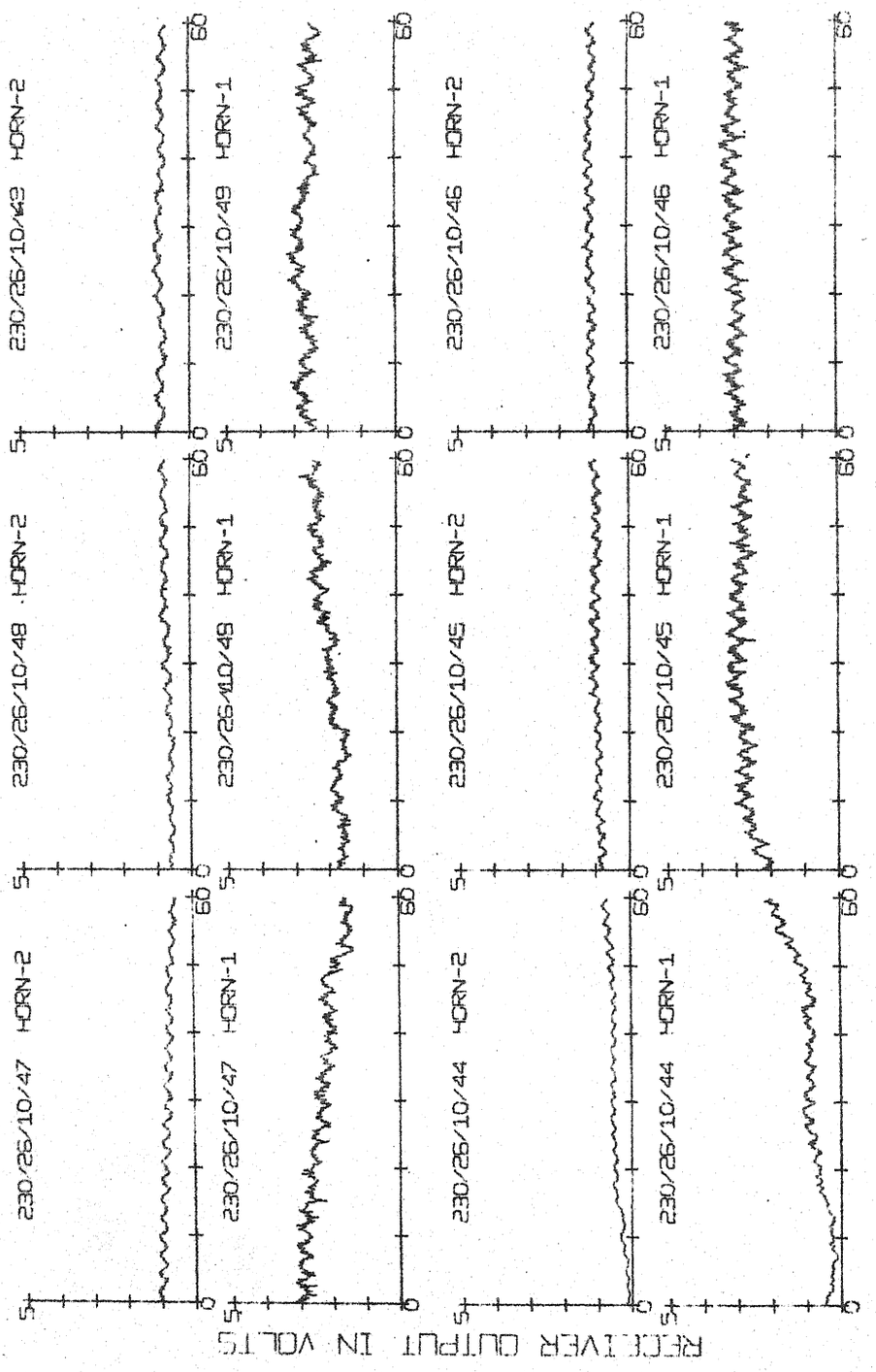

Fig.4.2 Night Time Signal

or where there was some unlocking of PLL between the 1 min sampling period were discarded and not taken into account for computation of correlation coefficient.

Since the set of samples taken from two horns were not for same instant of time, interpolation technique was applied to one of the sets of data, so that the values of samples at the same instant of time could be obtained for both horns. Use of sampling theorem was made to carry out this interpolation. The sampling theorem for stochastic processes is given by the relationship

$$X(t) = \sum_{n=-\infty}^{\infty} X(nT) \frac{\sin(\omega_c t - n\pi)}{\omega_c t - n\pi}$$

where X(t) is band limited and its spectrum satisfies the relation $S(\omega) = 0$ for $|\omega| > \omega_c$. With the values of X(nt) known, X(t) can be determined for any value of t. For the purpose of calculation, finite value of n was taken and only 10 samples were considered for finding the intermediate value.

For calculation of correlation coefficient between the two sets of samples the relationship

$$\rho = \frac{S_{xy}}{S_x S_y}$$ was used

where

$$S_x = \sum_{i=1}^{n} \frac{(x_i - \bar{x})^2}{n}$$

$$S_y = \sum_{i=1}^{n} \frac{(y_i - \bar{y})^2}{n}$$

$$S_{xy} = \sum_{i=1}^{n} \frac{(x_i - \bar{x})(y_i - \bar{y})}{n}$$

where n is the no. of samples and x_i, y_i are the instantaneous values of samples of signals received from two horns.

The correlation coefficient was found to have a mean values of .104 with a standard deviation of .152. A scattergram which shows the correlation of signal from horn 1 to those of horn 2 is shown in Fig. 4-3.

Programme 'COREL' which was developed to carry out data analysis is given in Appendix 'D'. Subroutine 'SORT' was developed to find the value of median received signals from both horns. Subroutine 'DEPTH' was developed to find the sample depth of fade in the two sets of signals. Subroutine 'SHIFT' was used to correct raw data for variation in the d.c. offset during the data logging operation.

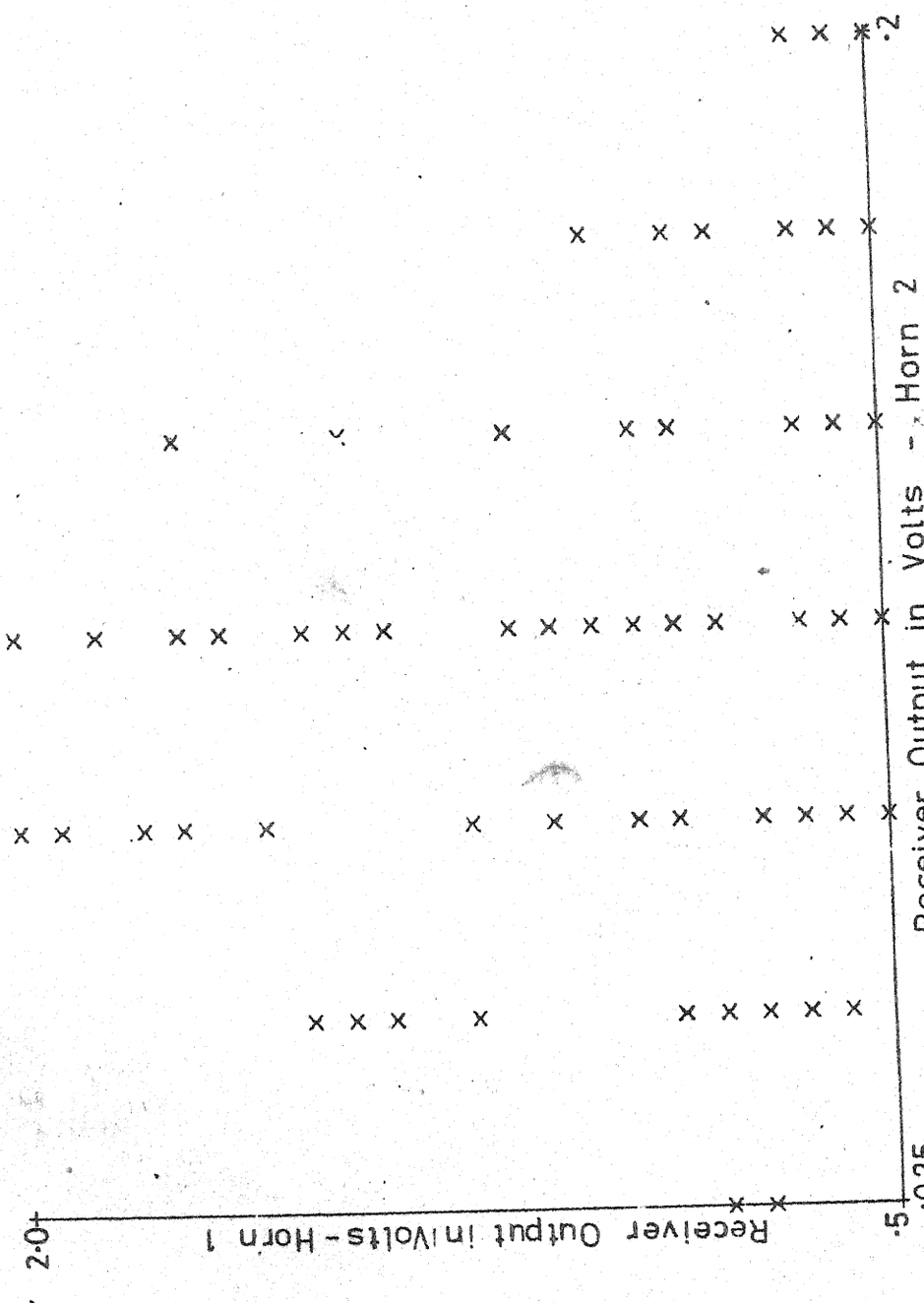

Fig. 4·3 Scattergram

Results of data analysis for 50 typical observations are tabulated in Table 2. The median received signals are found to have a mean value of -103 db and -110 db respectively. The difference in the mean values of median signals received from two horns is found to be 7 db.

TABLE 2

Time/Date/Month/Set	Median Received Signal		Depth of fade		Correlation coefficient
	Horn 1	Horn 2	Horn1	Horn2	
1500/1/11/1	-103	-110	8.2	5.3	-.217
1510/1/11/1	-103	-111	7.7	6.3	-.244
1515/1/11/1	-104	-110	7.6	7.1	-.177
1520/1/11/2	-105	-111	8.5	8.3	-.135
1520/1/11/1	-106	-111	9.2	7.3	-.154
1525/1/11/1	-104	-110	8.9	8.3	-.091
1210/2/11/1	-109	-114	12.1	4.7	-.252
1210/2/11/2	-106	-114	10.9	5.2	-.102
1255/2/11/1	-103	-109	9.6	5.7	-.009
1255/2/11/2	-104	-112	10.6	4.7	-.240
1255/2/11/3	-104	-114	11.9	7.1	-.170
1255/2/11/5	-102	-108	8.7	4.4	-.110
1255/2/11/6	-103	-112	10.6	9.0	-.017
1255/2/11/8	-99	-103	6.3	2.3	-.049
1255/2/11/9	-101	-108	8.2	3.3	-.056
1255/2/11/10	-104	-113	11.6	5.8	-.060
1255/2/11/12	-103	-115	11.6	7.3	-.248
1255/2/11/13	-103	-114	12.9	5.8	-.126
1255/2/11/14	-103	-111	11.6	5.8	-.176
1255/2/11/15	-100	-104	7.8	3.2	-.307
1255/2/11/16	-100	-113	11.6	7.7	-.149
1255/2/11/17	-102	-113	12.6	5.3	-.049
1255/2/11/19	-101	-111	11.6	6.0	-.170
1255/2/11/21	-101	-110	11.6	6.2	-.260
1255/2/11/24	-101	-111	11.6	5.0	-.150
1255/2/11/26	-102	-112	10.6	4.3	-.174

contd.....

Table 2 (contd.)

Time/Date/Month/Set	Median Received Signal		Depth of fade		Correlation coefficient
	Horn 1	Horn 2	Horn1	Horn2	
1255/2/11/27	-102	-111	12.6	5.6	-.114
1255/2/11/28	-102	-112	12.0	5.1	-.187
1255/2/11/29	-103	-111	11.6	5.0	-.174
1255/2/11/30	-102	-110	9.9	3.9	-.226
1255/2/11/31	-100	-108	11.6	3.6	-.114
1255/2/11/32	-103	-112	5.9	5.1	-.250
1255/2/11/33	- 98	-101	8.3	2.2	-.034
1255/2/11/34	- 99	-103	10.7	4.3	.173
1255/2/11/35	-101	-106	11.6	12.6	.519
1255/2/11/36	-101	-110	10.6	10.6	.337
1255/2/11/37	-102	-109	10.6	5.0	.0085
1255/2/11/38	-103	-111	11.6	4.8	.121
1255/2/11/39	-101	-108	8,6	4.6	.039
1255/2/11/40	-102	-109	8.5	4.9	.112
1700/3/11/2	-106	-113	10.0	7.4	-.097
1700/3/11/3	-106	-108	5.1	5.6	-.018
1500/4/11/9	-103	-111	9.1	8.1	-.232
1500/4/11/11	-105	-113	13.0	6.1	-.199
1500/4/11/13	-104	-113	11.3	7.3	-.204
1500/4/11/14	-105	-113	10.4	7.3	-.168
1500/4/11/15	-103	-109	9.1	5.9	-.141
1500/4/11/16	-103	-109	9.3	4.9	-.090
1500/4/11/17	-103	-109	8.4	4.6	-.147
1500/4/11/18	-103	-108	8.5	7.3	-.251
Mean	102.72	110.22	10.048	5.86	-.104
Standard Deviation	2.05	2.998	1.87	1.91	.152

CHAPTER 5

CONCLUSIONS AND SUGGESTIONS FOR FURTHER WORK

5.1 Conclusions:

In this experiment, angle diversity was achieved in a CW troposcatter experimental link between Kanpur and Nainital by utilising lateral displacement of feed horn of a paraboloidal antenna. For a transmitted power of +60 dbm, the mean value of median received signal strength (at the receiver input) via the main beam and the elevated beam, were found to be -102.72 dbm and -110.22 dbm respectively. (Feeder losses for the main horn was 16 db compared to 14 db for the displaced horn). The correlation coefficient between the median values of signals received from two horns were found to have a mean value of .104.

It is observed that the values of the median signal levels received from two horns are about 7 to 8 db lower than the long term medians predicted as per NBS 101 for the condition where both xmitting and receiving antennas are locally horizontal. (Appendix C). This was expected since most of the data collected was during the afternoon periods when the signal levels are comparatively low during winter months. Night time data was not included for the purpose

of analysis because the signal levels although very high, did not exhibit the characteristic Rayleigh fading. This phenomena has also been observed in the earlier experiments over this link, indicating that some anamolus mode of propogation is dominant during the night.

The difference of 7 db observed between the median signal levels from two horns compares favourably with the predicted difference of 6 db as per NBS-101.

The value of correlation coefficient is comparable with the largest value of 18.4% obtained by Vogelman, Ryerson and Bickelhaupt [3] and the mean value of .086 between horns 1 and 3 obtained by Monsen [5].

Thus it is concluded that vertical angle diversity configurations exhibit the low correlation necessary for effective diversity gain and angle diversity can provide a workable and economic alternative to other types of diversity.

5.2 Suggestions for Further Work:

Since the experiment was carried out over a limited period of time, the data obtained are not representative of conditions during all the seasons and all the hours of the day. The experiment will have to be extended to a

comparatively longer period to arrive at more accurate figures for long term medians of received signal strengths and long term correlations.

The seperation between the two horns was kept at 1λ, leading to an elevation of 1·8° for the displaced beam. A provision for changing the distance between the two horns has been made in the modified horn assembly. The closest distance to which the horns can be brought near to each other is limited by the dimensions of the horn mouth. Special feed horns will have to be designed for closer seperation. Narrower beamwidths can also be obtained by using larger antenna dishes.

As has been mentioned previously, the receiver set up that was used was originally designed for very long term troposcatter median path loss measurements and was subsequently used for this experiment with certain modifications. The receiver has a threshold sensitivity of -120 dbm so that for signal levels around -120 dbm, which are likely to be encountered during fades, the accuracy of recording is relatively low. This can be improved by front end noise figure reduction and 2nd IF B.W. reduction. For temperature stabilised oven controlled crystals of the type used in this receiver for generating the carrier and L.O. frequencies,

2nd IF bandwidth could be considerably reduced leading straight way to improvement in threshold sensitivity. Better OP amps could be used in the post detection circuitry to keep the d.c. drifts low, as this seriously limits the accuracy of the system while recording low level signals, this may however need readjustment of gain distribution among various stages of the system.

The signal acquisition and tracking capability of the P.L.L. can also be improved further, so that the switching can be done at a faster rate, enabling reproduction of signals with faster fading rates also without any aliasing errors. The faster switching rates for r.f. can be obtained by the use of PIN diodes.

APPENDIX A

DESIGN CONSIDERATIONS FOR FEED HORN

The primary radiator, usually a feed horn is designed to obtain the required taper of the aperture field. The effect of a non-uniform aperture distribution, with the amplitude tapering towards the edge of the aperture is to reduce the side lobes but at the expense of broader beamwidth and less antenna gain. The side lobe levels for various tapers are given in the table below.

Taper in db	Side lobe level in dbs (below main lobe level)
-6.0	-20
-11.0	-25
-14.5	-30
-17.5	-35

The optimum taper is a compromise between the beamwidth of the main lobe and the level of the side lobes due to excessive 'spill over'. Usually recommended figure for the optimum taper is about 8 to 12 db.

In terms of the half power beamwidth of a primary radiator (Fig. A.1), the taper due to the primary pattern can be expressed as

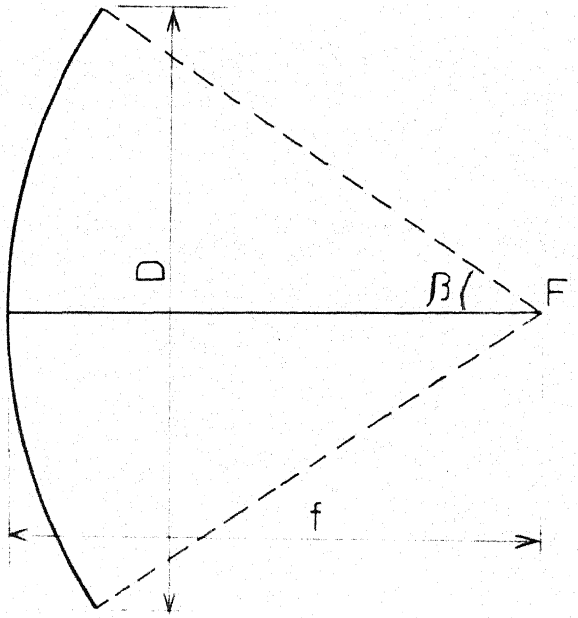

Fig.A1 Secondary Radiator Geometry

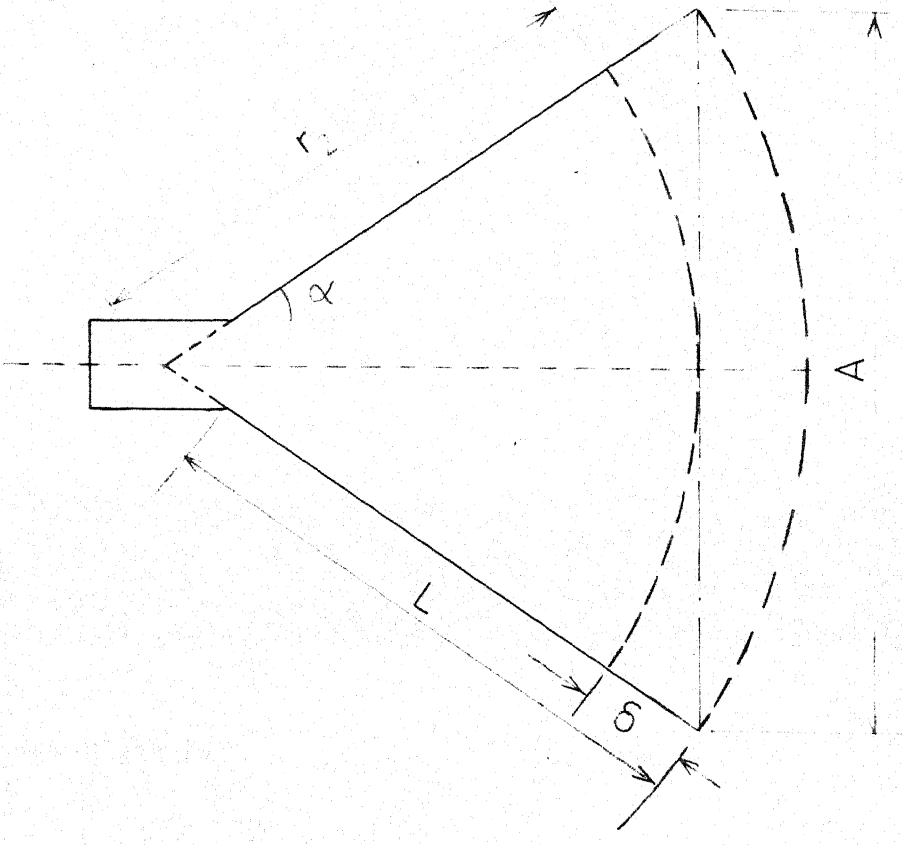

Fig. A 2 Horn Geometry

$$\tau_2 = -12 \left(\frac{\beta}{BW}\right)^2 \text{ db} \qquad \text{(A-1)}$$

The total taper in the aperture is the sum of the inherent taper τ_1 and the taper due to primary pattern τ_2. The inherent taper is due to the way in which the curvature of the reflector redistributes the power density in the aperture and may be evaluated as

$$\tau_1 = 40 \log \cos \beta/2 \qquad \text{(A-2)}$$

The dimensions of the mouth of the horn depend upon the beamwidth required.

Several empirical formulae have been worked out to calculate the horn dimensions from 3 db. beamwidth and also from the 10 db beamwidth [17].

If 10 db beamwidth in E plane $\theta_E(\frac{1}{10})$ and in H plane $\theta_H(\frac{1}{10})$ are known, then we have

(i) For the electrical plane

$$\theta_E(\tfrac{1}{10}) = \frac{88\lambda}{B} \text{ (degrees)}, \quad \frac{B}{\lambda} < 2.5 \qquad \text{(A-3)}$$

(ii) For the magnetic plane

$$\theta_H(\tfrac{1}{10}) = 31 + 79\,\frac{\lambda}{A}, \quad \frac{A}{\lambda} < 3.0 \qquad \text{(A-4)}$$

where B and A are apertures in the electrical and magnetic planes respectively. The flare angle of the average horn is probably around 20°.

Approximate formulae for the half power beamwidths of horns are

$$\theta_E(\tfrac{1}{2}) = \frac{56\lambda}{B} \qquad \text{(A-5)}$$

$$\theta_H(\tfrac{1}{2}) = \frac{67\lambda}{B} \qquad \text{(A-6)}$$

The selection of the length of the horn is related to the phase variation along the aperture of the horn. For a given aperture A, the phase variation δ is small, only if the flare angle α (Fig. A-2) is less than a maximum value (or the length r_2 is greater than a minimum value) which depends upon the aperture and can be obtained from the condition that δ/λ_g shall be small. Using the relation for the seperation of an arc and its chord, it is easily shown that

$$\frac{\delta}{\lambda_g} = \frac{D^2}{8r_2\lambda_g} = \frac{A \sin\alpha}{4\ \lambda_g} \qquad \text{(A-7)}$$

Using $\frac{1}{8}$ as the allowable upper limit for δ/λ_g

$$(r_2)\min = A^2/\lambda_g \qquad \text{(A-8)}$$

$$(\alpha)\ \max = \sin^{-1}\left(\frac{\lambda_g}{2A}\right) \qquad \text{(A-9)}$$

APPENDIX B

BEAM SCANNING WITH LATERAL DISPLACEMENT OF FEED HORN

1. Paraboloidal Reflector - Geometric Considerations

A paraboloidal reflector is a surface of revolution formed by rotating a parabola about an axis perpendicular to the parabola at its vertex. A paraboloid, symmetric with respect to x axis, with its vertex at the origin is shown in Fig. B-1.

The equation of this paraboloid is

$$y^2 + z^2 = 4fx \qquad \text{(B-1.1)}$$

In terms of the spherical coordinates (r,θ,ϕ) from the focal point shown in Fig. B-1 the equation of paraboloid is

$$r^2 = y^2 + z^2 = 4fx \qquad \text{(B-1.2)}$$

where f is the focal length of the paraboloid and

$$r^2 = \frac{2f}{1+\cos\psi} = f \sec^2(\psi/2) \qquad \text{(B-1.3)}$$

A section of the paraboloid in z=0 plane is shown in Fig. B.2.

Consider a ray from the focus, which strikes the parabola at the point (x_1, y_1).

The slope of the reflector can be found by differenciating eq. (B-1.1) for z=0.

This is $$\frac{dy}{dx} = \frac{2f}{y} = \tan\alpha \qquad \text{(B-1.4)}$$

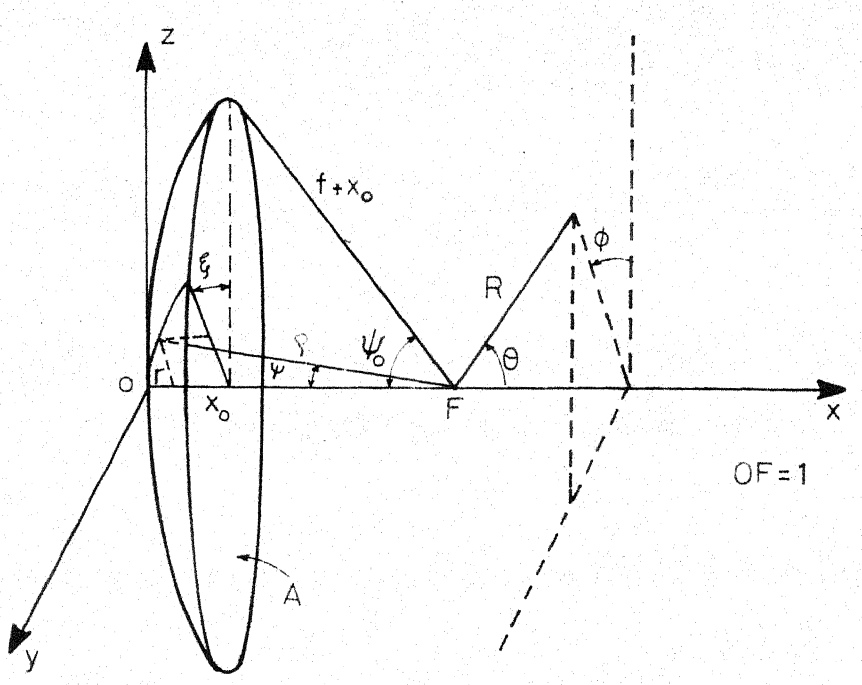

Fig. B-1 Paraboloid Geometry

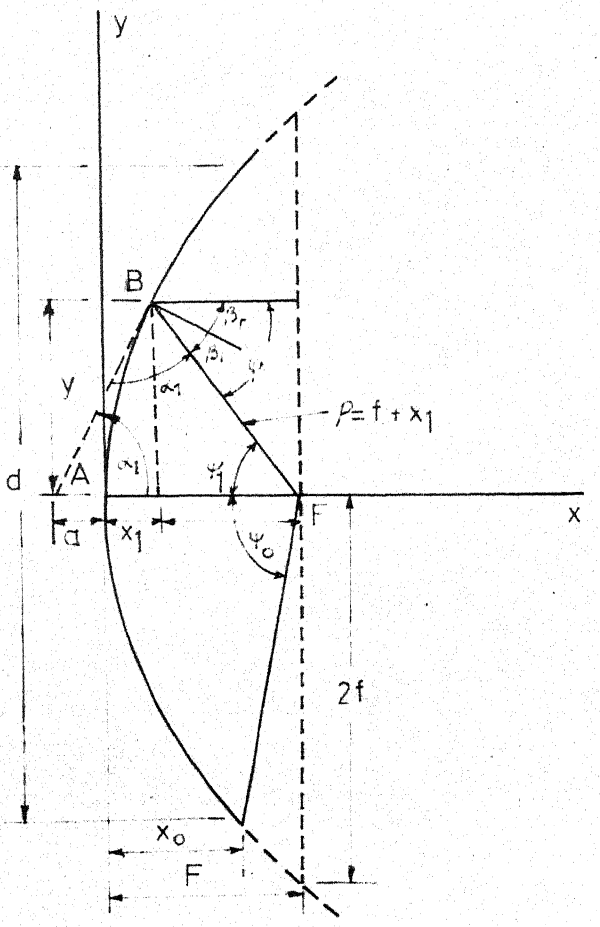

Fig. B-2 Sectional View of Paraboloid in x-y plane

The tangent to the point of reflection intersects the x axis at a distance 'a' behind the vertex, which can be found from

$$a+x_1 = \frac{y_1}{\tan \alpha_1} = \frac{y_1^2}{2f} = \frac{4fx_1}{2f} = 2x_1 \qquad \text{(B-1.5)}$$

Also the length of the ray from the focus to parabola is

$$\rho_1 = [(f-x_1)^2+y_1^2]^{1/2} = (f^2-2fx_1+x_1^2+4fx_1)^{1/2}$$

$$= f + x_1 \qquad \text{(B-1.6)}$$

Since the length of this ray is the same as the distance along the x axis from the focus to the intersection with the parabola tangent, traingle ABF is an isosceles traingle and the angle between the tangent and the ray from the focus is equal to the angle between the tangent and the x axis.

Therefore the angle of incidence at the reflector is given by

$$\beta_i = \frac{\pi}{2} - \alpha_i = \frac{1}{2}(\pi - 2\alpha_i) = \frac{\psi_1}{2} \qquad \text{(B-1.7)}$$

Since by Snell's law, the angle of incidence is equal to the angle of reflection, the angle between the incident and reflected rays at the reflector is equal to the angle between the incident ray and the x axis. The length of this ray from the focal point to the reflector and back to the line x=f is

$$r_1 = \rho_1 + (f-x_1) = 2f \qquad \text{(B-1.8)}$$

The shape of the reflector is also specified by angular aperture ψ, the angle between the x axis and the ray to the reflector. This angle is given by the relation

$$\tan \psi_1 = y_1/(f-x_1) \qquad \text{(B-1.9)}$$

The relation between angular aperture and the f/D ratio at edge of the dish is given by

$$\psi_o = \tan^{-1} \left[\frac{\frac{1}{2}(f/D)}{(\frac{f}{D})^2 - \frac{1}{16}} \right] \qquad \text{(B-1.10)}$$

The geometrical relations described above are useful for describing the performance of a parabolic reflector illuminated by a point source at the focus. However if the antenna primary feed has some artibrary distribution it is necessary to know the current distribution on the reflector or the fields in the secondary aperture to determine the antenna performance. The electric field for a constant phase aperture, with $\exp(-jkr)/kr$ and other nonpertinent factors deleted can be given in normalised form by the following equations [8].

$$F(u) = \frac{L}{2} \int_{-1}^{1} f(v)\, e^{juv}\, dv \qquad \text{(B-1.11)}$$

where $u = \frac{\pi L \sin\theta}{\lambda}$ and $v = \frac{2x}{L}$ where

the x variable is the distance along the line source from the centre, the source length is L and angle θ is measured from broad side.

f(v) = amplitude distribution over aperture

The far field pattern is the magnetude of F(u). However, when f(v) is an even function, the integral of eq. (B-1.11) is real and the pattern is simple F(u).

Two commonly used aperture distributions are

(i) Uniform - Electric field is constant in amplitude so f(v) = 1 which gives

$$F(u) = \frac{\sin u}{u} \qquad \text{(B-1.12)}$$

(ii) Cosine - $f(v) = \cos \frac{\pi v}{2}$

(considering first order cosine)

which gives

$$F(u) = \frac{L}{2} \int_{-1}^{1} \frac{\cos \pi v}{2} e^{juv} \, dv$$

$$= \frac{L}{\pi} \frac{\cos u}{1 - 4(\frac{u}{\pi})^2} \qquad \text{(B-1.13)}$$

2. Radiation pattern of parabolic reflector fed with Pyramidal Horn [8,12]

A paraboloid fed with horn is shown in Fig. B-3 where for convenience the paraboloid is cut to occupy a rectangular aperture with sides A and B in the y and z directions respectively. The horn is fed by a rectangular

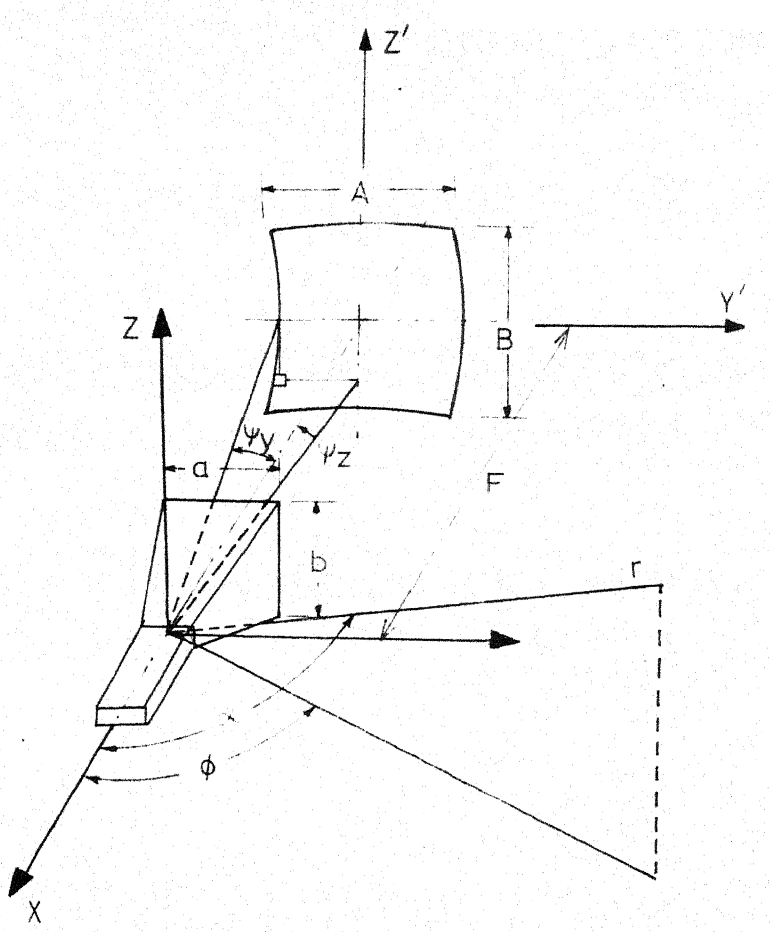

Fig B-3 Paraboloid fed with Horn

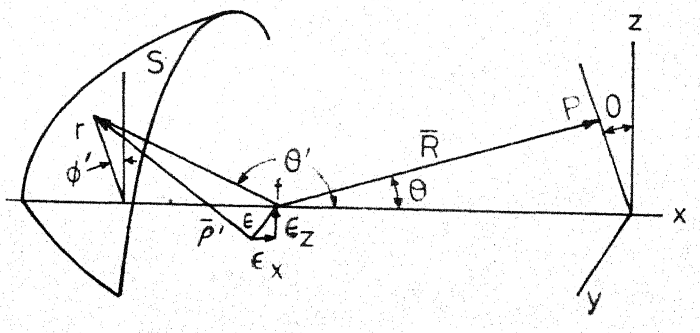

Fig. B-4 Coordinate System

waveguide which is excited only in the dominant mode TE_{10}. This will give a uniform field in the E plane and a tapered field in the H plane.

For a uniform field, the E plane pattern of the horn feed for a horn height b is

$$f_E = \frac{\sin\left[\frac{kb}{2}\sin\psi_z\right]}{\left[\frac{kb}{2}\sin\psi_z\right]} = \sin\frac{U_E}{U_E} \qquad \text{(B-2.1)}$$

where $U_E = \frac{kb}{2}\sin\psi_z$

Presuming a first order cosine distribution, the H plane pattern of the horn field is

$$f_H = \frac{\cos U_H}{1-4\left(\frac{U_H}{\pi}\right)^2} \quad \text{where } U_H = \frac{\pi a}{\lambda}\sin\psi_y$$

Illumination of the dish at any point in E plane and H plane is given by

$$f_E(z) = \sin\frac{\sin\left[\frac{\pi b}{\lambda}\sin\tan^{-1}\frac{z}{f-x_o}\right]}{\frac{\pi b}{\lambda}\sin\left(\tan^{-1}\frac{z}{f-x_o}\right)} \qquad \text{(B-2.3)}$$

$$f_H(y) = \frac{\cos\left[\frac{\pi a}{\lambda}\sin\left(\tan^{-1}\frac{y}{f-x_o}\right)\right]}{1-4\left[\frac{a}{\lambda}\sin\left(\tan^{-1}\frac{y}{f-x_o}\right)\right]} \qquad \text{(B-2.4)}$$

The fields from the dish for secondary patterns are fourier transforms of the distribution of the fields at its aperture.

Taking into account the finite diameter D of the reflector we have

$$E_E = \int_{-D/2}^{+D/2} f_E(z)\, e^{jkz \sin \alpha} dz \qquad \text{(B-2.5)}$$

$$E_H = \int_{-D/2}^{+D/2} f_H(y)\, e^{jky \sin \alpha} dy \qquad \text{(B-2.6)}$$

3. Power patterns for different feed displacements [11]

The field at a far point with feed at the focus is given in spherical coordinates as

$$E(\theta,\phi) = \int_0^{2\pi} \int_0^{a} f(r,\phi')e^{jk\,(\bar{\rho} - \bar{\rho}\,.\,\bar{R}_o)}\, r\, dr d\phi'$$

where aperture diameter D = 2a (B-3.1)

$f(r,\phi')$ is effective aperture distribution and all constant factors are suppressed. Bars represent vector quantities and the subscript 'o' their unit values.

Let the displacement of feed be ε as shown in Fig. B-3.

With displacement of feed the field at the far point changes to

$$E(\theta,\phi) = \int_0^{2\pi} \int_0^{a} f(r,\phi')e^{jk\,(\bar{\rho}' - \bar{\rho}'\,.\bar{R}_o)}\, r\, dr d\phi' \qquad \text{(B-3.2)}$$

Here we have assumed that the magnitude of the effective aperture distribution has remained unchanged. This implies that the vertix ray is the principal ray. The feed should therefore be pointed at the vertex.

From the figure we have

$$\rho = \frac{2f}{1-\cos\theta'} = \frac{2f}{1+\cos\psi} = f \sec^2 \frac{\psi}{2} \qquad \text{(B-3.3)}$$

$$\bar{\rho} = \rho [\cos\theta' \bar{x} + \sin\phi' \sin\theta' \bar{y} + \cos\phi' \sin\theta' \bar{z}] \qquad \text{(B-3.4)}$$

$$\bar{R}_o = [\cos\theta \bar{x} + \sin\phi \sin\theta \bar{y} + \cos\phi \sin\theta \bar{z}] \qquad \text{(B-3.5)}$$

$$\bar{\rho}' = \bar{\rho} + \varepsilon_x \bar{x} + \varepsilon_z \bar{z} \qquad \text{(B-3.6)}$$

$$= [1 + \frac{2\varepsilon_x}{\rho} \cos\theta' + \frac{2\varepsilon_z}{\rho} \cos\phi' \sin\theta' + \frac{\varepsilon^2}{\rho^2}]^{1/2} \qquad \text{(B-3.7)}$$

Neglecting higher order terms of $\frac{x}{\rho}$ and $\frac{z}{\rho}$

as $\frac{\varepsilon_x}{\rho} < \frac{\varepsilon_x}{f} << 1$

the phase factor of eq. (3.30) is given as

$$\rho' - \bar{\rho}' \bar{R}_o = [2f - \varepsilon_z \cos\phi \sin\theta - \varepsilon_x \cos\theta] -$$
$$[\rho \sin\theta' \sin\theta \cos(\phi'-\phi)] + [\varepsilon_z \cos\phi' \sin\theta']$$
$$+ [\varepsilon_x \cos\theta' + \frac{\varepsilon_z^2}{2\rho} + \rho \cos\theta' (1-\cos\theta)] -$$
$$[\varepsilon_z/2\rho (\cos^2\phi' \sin^2\theta')] \qquad \text{(B-3.8)}$$

In the above equation, first three terms are independent of the integration coordinates and may be taken out of

integral and included in constant factor. They represent a phase pattern of the field. As $r = \rho \sin\theta'$, the normal phase factor due to an inphase aperture is given by the fourth factor. The fifth term represents the phase error factor, which encompasses linear, cubic and higher order odd powers of integration coordinate. This provides the beam shift and comatic aberration.

The next three terms are proportional to r^2 and higher order even power terms which can be eliminated by refocussing the feed. The last term is the astigmatism Refocussing condition gives the petzvel surface, a term from optics, which is defined as the surface of best focus in an optical systen in absence of astigmation. Setting the field curvature and higher order even power terms to zero, we get locus of feed as

$$\epsilon_x = \frac{\epsilon_z^2}{2f} \qquad \text{(B-3.9)}$$

Therefore for sharpest null, the feed locus for small aberration is defined by eq. (3.37) as another paraboloid of focal length f/2, tangent to the focal plane. The vertex feed distance must therefore be slightly increased as we scan off axis.

With feed in the optimum position and neglecting the astigmation in comparison to comatic aberration, the magnitude of the far field can be written as

$$E(\theta,\phi) = \int_0^{2\pi} \int_0^{a} f(r,\phi') e^{-jk\left[r\sin\theta\cos(\phi'-\phi)-\varepsilon_z\sin\theta'\cos\phi'\right]} r\,dr\,d\phi \qquad \text{(B-3.10)}$$

This can be further simplified as

$$E(\theta,\phi) = \int_0^{2\pi} \int_0^{a} f(r,\phi') e^{jkr\,A\cos(\phi'-\alpha)}\, r\,dr\,d\phi' \qquad \text{(B-3.11)}$$

where $A = u^2 - \dfrac{2u\,u_s}{M(r)}\cos\phi + \dfrac{u_s^2}{M^2(r)}$

$$\tan\alpha = \frac{u\sin\phi}{u\cos\phi - \dfrac{u_s}{M(r)}}$$

$u = \sin\theta$

$u_s = \varepsilon_z/f$ = feed squint

$M(r) = 1 + (r/2f)^2$

For circularly symmetrical illumination functions, the ϕ' integration can be performed with the result

$$E(\theta,\phi) = 2\pi \int_0^{a} f(r)\, J_o\,(krA)\, r\,dr \qquad \text{(B-3.12)}$$

Equation (B-3.12) can be evaluated for specified illumination. For the illumination given in the E plane and H plane

respectively by eqs. (B-2.3) and (B-2.4). Equation (B-3.12) yields on normalisation and dropping all constants

$$E_E = \int_0^1 f_E(z)\, J_o(kzA)\, z\, dz \qquad \text{(B-3.13)}$$

$$E_H = \int_0^1 f_H(y)\, J_o(kyA)\, y\, dy \qquad \text{(B-3.14)}$$

Power patterns for E plane and H plane, with different displacements of feed have been calculated and plotted by Swarnkar [15], for a pyramidal feed horn of the same dimensions as used in this experiment. The E plane pattern is reproduced in Figure B.5.

It is seen from the patterns that for a feed displacement of 1λ, the main beam is displaced by an angle of approx. 1.8^{o}.

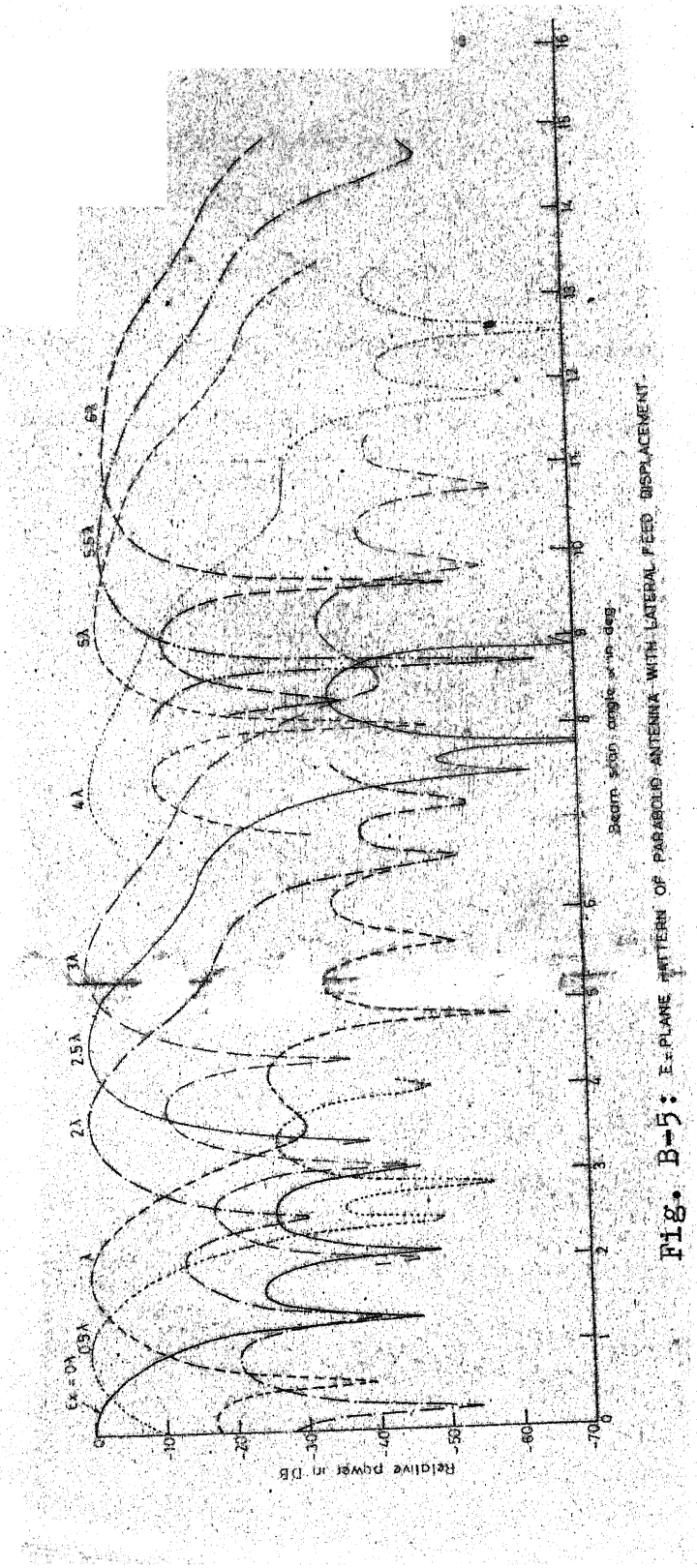

Fig. B-5: E-PLANE PATTERN OF PARABOLOID ANTENNA WITH LATERAL FEED DISPLACEMENT

APPENDIX C

PATH LOSS CALCULATIONS

The troposcatter path loss for the main beam as well as the elevated beam was calculated in accordance with section 9 of NBS Technical Note 101.

The required inputs are as follows:

Operating frequency	$f = 2.1$ GHzs.
Path length	$d = 325.75$ kms.
Surface refractivity	$N_s = 290$
Height of centre of Transmitting antenna above sea level	$ht_s = 6390$ ft $= 1.9476$ kms.
Height of centre of receiving antenna above sea level	$hr_s = (415+40)$ft. $= .1386$ km.
Height of Transmitter horizon obstacle above sea level	$h_{Lt} = 0$ km
Height of Receiving horizon obstacle above sea level	$h_{Lr} = 0$ km
Effective earth radius	$a = a_o[1-.04665 \exp(.005577\ N_s)]^{-1}$
	$= 8327.86$ for $N_s = 290$

A typical troposcatter path geometry is shown in Fig. C-1.

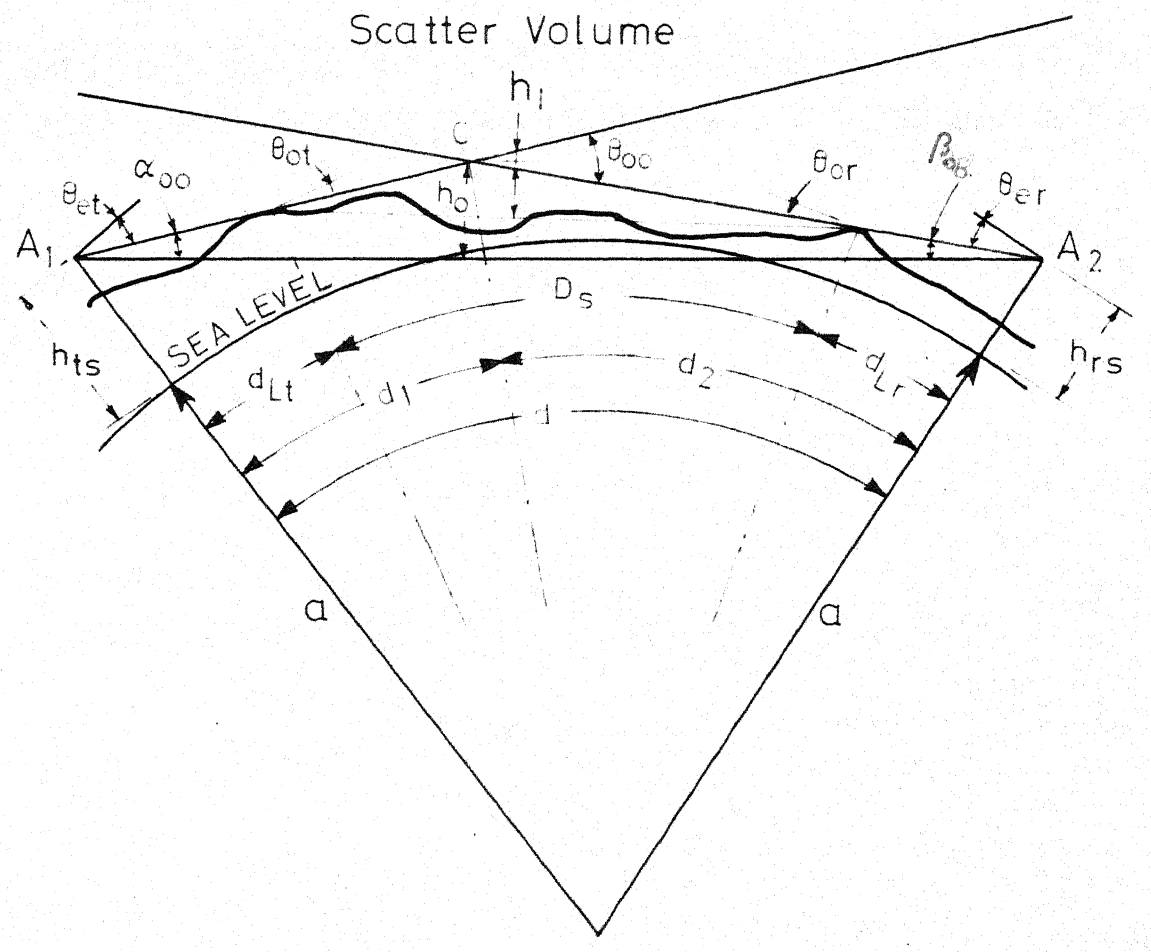

Distances are measured in kilometers along a great circle arc

$$\theta_{oo} = \frac{D_s}{a} + \theta_{ot} + \theta_{or} = \frac{d}{a} + \theta_{et} + \theta_{er}$$

Fig. C1 Typical Troposcatter Path Geometry

C.I. Calculation of Effective Antenna Heights ht_e and hr_e

$\bar{h}_t = \bar{h}_r = 0$

$h_t = ht_s - \bar{h}_t$ for $\bar{h}_t < ht_o$

$h_r = hr_s - \bar{h}_r$ for $\bar{h}_r < hr_o$

$ht = ht_s = 1.9476$ km

$h_r = hr_s = .1386$ km

$\Delta h_e\ (h_t, N_s = 290) = .009$ km for $N_s = 290$ (Fig. 6.7 NBS 101)

Effective Transmitting Antenna Height

$ht_e = h_t - \Delta h_e = 1.9386$ km

Effective Receiving Antenna Height

$hr_e = hr_s = .1386$ km.

C.II : Calculation of Path Angular Distances

(Transmitting and Receiving antennas both locally horizontal)

θ_{et} = Elevation angle at the transmitter

$= 0$

θ_{er} = Elevation angle at the receiver for the main beam

$= 0$

dL_t = Great circle distance from the transmitting antenna to corresponding horizontal obstacle

$= 0$

dL_r = Great circle distance from the receiving antenna to corresponding horizontal obstacle

$= 0$

α_{oo} = angle between a transmitter horizontal ray and a line drawn between the antenna locations on an earth of effective radius 'a'

$= \frac{d}{2a} + \theta_{et} + \frac{ht_s - hr_s}{d} = 25.1$ m rads

β_{oo} = angle between a receiver horizontal ray and a line drawn between the antenna locations on an earth of effective radius 'a'

$= \frac{d}{2a} + \theta_{er} + \frac{hr_s - ht_s}{d} = 14.0$ m rads.

$\theta_{oo} = \alpha_{oo} + \beta_{oo} = 39.1$ m rads.

ds_t = Distance between transmitting antenna horizon and the crossover of transmitter horizontal ray and receiver horizontal ray

$= \frac{d\beta_{oo}}{\theta_{oo}} - dL_t = d\beta_{oo}/\theta_{oo} = 116.6$ km

ds_r = Distance between receiving antenna horizon and the crossover of transmitter horizontal ray and receiver horizontal ray

$= \frac{d\alpha_{oo}}{\theta_{oo}} - dL_r = \frac{d\alpha_{oo}}{\theta_{oo}} = 209.1$ km

θ_{ot} = angular elevation of a horizontal ray at the transmitter horizon

$= \theta_{et} + \frac{dL_t}{a} = 0$

θ_{or} = angular elevation of a horizontal ray at the receiver horizon.

$= \theta_{er} + \frac{dL_r}{a} = 0$

$\Delta\alpha_o$ = correction factor used to compute α_o

= 0 (Fig. 6.9 of NBS 101 Part I)

$\Delta\beta_o$ = correction factor used to compute β_o

= 0 (Fig. 6.9 of NBS 101 Part I)

α_o = Angle α_{oo} modified by correction factor $\Delta\alpha_o$

= 25.1 m rads

β_o = Angle β_{oo} modified by correction factor $\Delta\beta_o$

= 14.0 m rads

θ = Path angular distance between xmitter horizontal ray and receiver horizontal ray

= $\alpha_o + \beta_o = 39.1$ m rads.

S = Path assymetry factor

= $\frac{\alpha_o}{\beta_o} = 1.79$

β'_o = β_o + 31.428 m rads

= 45.4 m rads.

θ' = Path angular distance between transmitter horizontal ray and receiver upper ray (corresponding to displaced horn)

= $\alpha_o + \beta_o' = 70.5$ m rads

S' = Path assymetry factor for upper ray

= $\alpha_o / \beta_o' = .55$

C-III: <u>Calculation of Long term median transmission loss for main beam</u> :

θd = 12.74

$F(\theta d)$ = [135.82+.33 θd + 30 log (θd)]

= 173.64

$F(\theta d, N_s) = F[\theta d, N_s = 301] - [0.1(N_s - 301)e^{-\theta d/40}]$

$= 174.44$ dB for $N_s = 290$

D_s = Great circle distance between transmitting and receiving horizons

$= d - dL_t - dL_r = d$

$= 325.75$ km

H_o = Frequency gain function

$= 0$ since $\frac{ht_e}{\lambda} > \frac{4a}{d}$ and $\frac{hr_e}{\lambda} > \frac{4a}{d}$

h_o = Height of intersection of horizon rays above a straight line between the antennas, determined using effective earth radius a

$= S\, d\theta/(1+S)^2$ km $= 2.9285$ km

$\eta_s = .5696\, h_o\, [1+(.031-2.32N_s x10^{-3}+5.67N_s^2 \times 10^{-6}) x \exp(-3.8h_o^6 \times 10^{-6})]$

$= 1.39$

h_1 = Height of the crossover of horizon rays above a straight line between the transmitter and receiver horizons obstacles

$= S\, D_s\theta/(1+S)^2$ km $= 2.92$ km as $D_s = d$.

F_o = Correction term for reduction of scattering effeciency at great heights in atmosphere

$= 1.086(\eta_s/h_o)(h_o - h_1 - hL_t - hL_r)$ dB

$= 0$

A_a = Long term median attenuation of radio waves due to atmospheric absorption by oxygen and water vapour

= 1.65 db (Fig. 3.6 of NBS 101 Part I)

L_{bsr} = Long term median basic transmission loss due to forward scatter

= 30 log f - 20 log d + $F(\theta d) - F_o + H_o + A_a$ dB

= 224 db

d_e = Effective distance in km

= $130 + d - [3\sqrt{2ht_e} + 3\sqrt{2\,hr_e} + 65(100/f)^{1/3}]$

= 195.4 km

$V_n(0.5, d_e)$ = Correction factor depending on climatic region and effective distance

= 3.5 db (Fig. 10.13 of NBS-I assuming continental subtropical climate)

$L_n(0.5)$ = Predicted long term median transmission loss for the climatic region in question

= $L_{bsr} - V_n(0.5, d_e)$

= 220.5

C-IV: <u>Calculation of long term median transmission loss for elevated beam</u>:

$\theta' d$ = 22.98

$F[\theta', d]$ = 184.24 db

$F[\theta' d, N_s]$ = 184.86 db for N_s = 290

D_s = 325.75 km

h_o' = Height of crossover of the transmitter horizontal ray and receiver elevated ray, above a straight line between the antennas.

= $S'\, d\theta'/(1+S)^2$ km

= 5.26 km

H_o' = Frequency gain function

= 0

$$s' = .5696\, h_o' \left[1+(.031-2.32N_s x10^{-3} +5.67\, N_s^2 \times 10^{-6}) \exp(-3.8\, h_o'^6 \times 10^{-6})\right]$$

= 2.68

h_1' = Height of cross-over of transmitter horizontal ray and receiver elevated ray, above a straight line between the transmitter and receiver horizontal obstacles.

= $S'D_s\theta'/(1+S)^2$ km

= h_o' = 5.27

F_o = $1.086(\eta_s'/h_o')\ (h_o'-h_1'-hL_t-hL_r)$ db

= 0 since $h_o' = h_1'$ and $hL_t=hL_r$.

A_a = 1.65 db

L_{bsr} = 236 db

$L_n(0.5)= L_{bsr}-V_n(0.5\, d_e)$ dh

= 236 - 3.5 db

= 232.5 db

C-V Calculation of Receiver Input from Horn-1 (middle horn)

Calculation of L_{gp} (Forward scatter multipath coupling loss).

$$\nu = \frac{\eta_s}{2} = .69$$

$$f(\nu) = [1.36 + .116\nu][1+0.36 \exp(-0.56)]^{-1}$$

$$= 1.16$$

$$\delta_r = \delta_t = \frac{56\lambda}{D} = .016 \quad \text{radians}$$

$$\mu = \frac{\delta_r}{\delta_t} = 1$$

$$s\mu = 1.8 \qquad \frac{1}{s\mu} = .55$$

$$n = \frac{\alpha_o}{\delta_r} = 1.53$$

$$n = (n+.03\nu)/f(\nu)$$

$$= 1.34$$

$$L_{gp} = 5 \text{ db (Fig. 9.8 NBS I)}$$

Calculation of free space power gains of xmitting and receiving antennas:

$$G_t = G_r = (20 \log D + 20 \log f - 42.10)\text{db} = 43 \text{ db}$$

where D is in meters

f is in MHzs

56 % aperture efficiency is assumed

Feeder and mismatch losses - $L_L = 16$ db

RF Transmission loss factor

$$L_T = L_h(0.5) + L_{gp} + L_L - G_t - G_r$$

$$= 220.5 + 5 + 15 - 86$$

$$= 155.5$$

Signal at receiver input from horn 1 = - 95.5 dbm

C-VI Calculation of Receiver Input from Horn-2 (Displaced horn)

Calculation of L_{gp}

$$\nu' = \frac{n's}{2} = 1.34$$

$$f(\nu') = 1.3$$

$$\delta_r = \delta_t = .016 \quad \text{radians}$$

$$\mu = 1$$

$$s'\mu = .55$$

$$\frac{1}{s'\mu} = 1.8$$

$$n = \frac{\beta_o'}{\delta_r} \quad \text{for } s'\mu \leq 1$$

$$= 2.77$$

$$n = (n + .03\,\nu')/f(\nu')$$

$$= 2.17$$

$$L_{gp} \approx 9 \text{ db}$$

Calculation of G_t and G_r

$$G_t = G_r = 42 \text{ db}$$

(assuming that the gain is 1 db lower than for the main beam)

Feeder and mismatch losses

$$L_L = 4 \text{ db}$$

RF transmission loss factor

$$L_T = 161.5 \text{ db}$$

Signal at receiver input from horn 2

$$= -101.5 \text{ dbm}$$

C-VII Difference between Signals from Horn 1 and Horn 2

Predicted difference $\approx$ 6 db

APPENDIX - D

SOFTWARE

PROGRAM 'DATLG' FOR DATA LOGGING

```
// JOB
// FOR DATLG
C       DIFFERENT MODES OF OPERATION DEPENDING ON SENSE SWITCH POSITION
C       SS-SE SWITCH 5 TO BE UP ONLY WHEN DESIRED TO STOP DATA LOGGING
C       SS-SE SWITCH 2 AND 3 TO BE UP FOR AUTOMATIC DATALOGGING
C       IF SS-SE SWITCH 4 UP  2 SECS DELAY BETWEEN DIFFERENT SETS
C       IF SS-SE SWITCH 4 DOWN THEN 90 SECS DELAY BETWEEN SETS
C       SS-SE SWITCH 2 DOWN DATALOGGING CONTROLLED BY KEYBOARD
C       IF SS-SE SWITCH 3 UP WHEN SENSE SWITCH 2 IS DOWN THEN NO TAPING
*LOCS(CARD,TYPEWRITER,MAGNETIC TAPE)
*-3 PROCESS PROGRAM
*-3 DEFINE INTEGERS
      DIMENSION IDTA(600),IDTB(600)
      COMMON IDTA,IDTB,MONTH,ITIME,IDAY,ISET
      DATA IDOLR/'SS'/
      DATA II,JJ/21,13/
C     SCANNING FOR LAST DATA RECORDED IN TAPE
      READ(4,)
      IF(J-IDOLR)6,12,6
   12 CALL SSWTCH(2,LNDIC)
      GO TO (1003,1002),LNDIC
 1003 WRITE(1,100)
  100 FORMAT('ENTER TIME,DATE,MONTH,OO  IN FORMAT I4,3I2')
      CALL BUSY
      READ(2,45) ITIME,IDAY,MONTH,ISET
```

```
   45  FORMAT(I4,3I2)
       CALL BUSY
 1011  DO350 I=1,2000
       DO350 J=1,1000
  350  CONTINUE
       GO TO 1004
 1002  PAUSE123
 1004  CALL SSWTCH(5,INDIC)
       GO TO (1006,1009),INDIC
 1009  J=1
       K=1
       DO300 I=1,600
       IDTA(I)=0
  300  IDTB(I)=0
C      READING THE ANALOG INPUT POINT
       DO200 I=1,120
       CALL AIE(0110O,IDATA,4111)
       CALL AIE(0,ITEST)
       GO TO (10,20),ITEST
   20  CONTINUE
C      PROGRAMME CONTROLLED DELAY BETWEEN CONSECUTIVE ANALOG INPUT READING
       DO1001 L=1,10
       DO1001M=1,JL
 1001  CONTINUE
C      SORTING ODD AND EVEN SAMPLES INTO DIFFERENT ARRAYS
       IF(I-I/2*2) 101,100,101
  100  IDTA(J)=IDATA
       J=J+1
       GO TO 200
  101  IDTB(K)=IDATA
       K=K+1
  200  CONTINUE
       CALL SSWTCH(2,INDIC)
       GO TO (152,151),INDIC
C      RECORDING THE DATA INTO TAPE
```

```
151   PAUSE123
      CALL SSWTCH(3,INDIC)
      GO TO(1002,1005),INDIC
1005  CALL TAPNG
      GO TO 1002
152   CALL TAPNG
      CALL SSWTCH(4,INDIC)
      GO TO (1007,1011),INDIC
1007  DO450 J=1,40
      DO450 J=1,1000
450   CONTINUE
      GO TO 1004
1006  REWIND 4
      CALL EXIT
      END
```

SUBROUTINE 'TAPNG'

```
// FOR TAPNG
      SUBROUTINE TAPNG
      DIMENSION IDTA(600),IDTB(600)
      DATA IDOOR/'$$'/
      COMMON IDTA,IDTB,MONTH,ITIME,IDAY,ISET
      CALL SSWTCH(2,INDIC)
      GO TO (25,24),INDIC
   24 WRITE(1,23)
   23 FORMAT('ENTER TIME,DATE,MONTH,SET I. FORMAT I4,3I2')
      CALL HOST
      READ(2,15)ITIME,IDAY,MONTH,ISET
      GO TO 26
   25 ISET=ISET+1
   26 BACKSPACE 4
      WRITE(4) ITIME,IDAY,MONTH,ISET
      WRITE(4)IDTA,IDTB
      WRITE(4)ITIME,IDAY,MONTH,ISET
      WRITE(4) IDOOR
      WRITE(1,15)ITIME,IDAY,MONTH,ISET
   15 FORMAT('DATA TAPED',10X,I4,'HOURS',I2,'-',I2,'-79 SET-',I2)
      RETURN
      END
```

PROGRAM "CORE1" FOR DATA ANALYSIS

```
// JOB
// FOR COREL
*IOCS(CARD,TYPEWRITER,MAGNETIC TAPE,PLOTTER)
* 0- PROCESS PROGRAM
*LIST WORD INTEGERS
      DIMENSION M(600),N(600)
      COMMON M,
       I=600
       I=I-5
       I=I-10
      IF(I-4
      CALL SSWTCH(2,INDIC)
      GO TO (1003,1002),INDIC
 1002 PI=3.14159265
      WRITE(1,45)
   45 FORMAT('PRINT TIME DAY MONTH SETFOR REQD. PLOT IN I4,3I2')
      CALL BUSY
      READ(2,10)ITIME,IDAY,MONTH,ISET
   10 FORMAT(4I,312)
   25 READ(4)JTIME,JDAY,JMONT,JSET
      IF(J-MONT-MONTH) 30,40,30
   40 IF(JDAY-IDAY)30,50,30
   50 IF(JTIME-ITIME)30,60,30
   60 IF(JSET-ISET)30,70,30
   70 READ(4)M,N
      READ(4)JTIME,JDAY,JMONT,JSET
      GO TO 130
   30 READ(4)M,N
      READ(4)JTIME,JDAY,JMONT,JSET
      GO TO 25
```

```
 33   CONTINUE
      WRITE(1,20)JTIME,JDAY,JJOBT
 20   FORMAT('DATA ANALYSIS FOR',2X,I4,'HOURS ON',2X,I2,'-',I2,'-79'//)
      WRITE(1,35)JSET
 35   FORMAT(5X,'SET NUMBER=',5X,I2//)
      CALL BUSY
      CALL SHIFT(M,N)
      A1=2./PI
      A2=2./(3.*PI)
      A3=2./(5.*PI)
      A4=2./(7.*PI)
      A5=2./(9.*PI)
      DO200 K=6,NM
      KE=K-3
      KG=K-2
      KM=K-1
      KI=K-4
      KJ=K-1
      KK=K+1
      KL=K+2
      KM=K+3
      KN=K+4
      M(KF)=M(KJ)
200   M(K)=A1*FLOAT(M(K)+M(KJ))-A2*FLOAT(M(KI)+M(KK))
     *+A3*FLOAT(M(KL)+M(KJ))-A4*FLOAT(M(KG)+M(KM))+A5*FLOAT(M(KF)+M(KN))
      SUMX=0.
      SUMY=0.
      SUMXY=0.
      SUMY2=0.
      SUMX2=0.
      DO350 I=1,NM
      A=FLOAT(M(I))
      B=FLOAT(N(I))
      SUMX=SUMX+A
      SUMY=SUMY+B
```

```
      SUMXY=SUMXY+A*B
      SUMX2=SUMX2+A*A
  350 SUMY2=SUMY2+B*B
      P=AN
      CURCO=(SUMXY-(SUMA*SUMY/P))/SQRT((SUMX2-SUMX*SUMA/P)
     **(SUMY2-SUMY*SUMY/P))
      WRITE(1,65)CURCO
   65 FORMAT('CORRELATION COEFFICENT=',5X,E15.8///)
      CALL SORT(4,MEDL1)
      CALL SORT(5,MEDL2)
      WRITE(1,250)MEDL1
      WRITE(1,255)MEDL2
  255 FORMAT('MEDIAN RECEIVED SIGNAL LEVEL HORN 2=',5X,I5,'DBM'//)
  250 FORMAT(' MEDIAN RECEIVED SIGNAL LEVEL HORN 1=',5X,I5,'DBM'//)
      CALL DEPTH(4,FADE1)
      CALL DEPTH(5,FADE2)
      WRITE(1,300)FADE1
  300 FORMAT('SAMPLE DEPTH OF FADE HORN1=',5X,F6.1,'DBM'//)
      WRITE(1,310)FADE2
  310 FORMAT('SAMPLE DEPTH OF FADE HORN2=',5X,F6.1,'DBM'//)
      READ(4)DIFFE,SUM1,SUMAT,SUM1
      GO TO 70
  100 CALL EXIT
      END
```

SUBROUTINE 'SORT'

```
// FOR SORT
      SUBROUTINE SORT(IBUFF,MEDNR)
      DIMENSION IBUFF(600)
      COMMON NL
      N=NL
   10 N=N/2
      IF(N)70,70,20
   20 K=NL-N
      J=1
   30 I=J
   40 L=I+N
      IF(IBUFF(I)-IBUFF(L))60,60,50
   50 ITEMP=IBUFF(I)
      IBUFF(I)=IBUFF(L)
      IBUFF(L)=ITEMP
      I=I-N
      IF(I-1)60,40,40
   60 J=J+1
      IF(J-K)30,30,10
   70 CONTINUE
C     CALCULATION OF MEDIAN RECEIVED SIGNAL
      MN=NL/2
      MEDN1=IBUFF(MN)
      MN=(NL/2)+1
      MEDN2=IBUFF(MN)
      MEDN=(MEDN1+MEDN2)/2
      X=(FLOAT(MEDN)*5.)/8186.
      DBX=20.*(ALOG(X)/2.303)-88.
      MEDNR=DBX
      RETURN
      END
```

SUBROUTINE 'DEPTH'

```
// FOR DEPTH
      SUBROUTINE DEPTH(A,DEPAD)
      DIMENSION M(600)
      COMMON ML
      II=ML/10
      X=M(II)
      X=X*5./6186.
      TEMPL=20.*(ALOG(X)/2.303)-88.
      JJ=9*II/10
      X=M(JJ)
      X=X*5./6186.
      TEMPH=20.*(ALOG(X)/2.303)-88.
      DEPAD=TEMPH-TEMPL
      RETURN
      END
```

PROGRAM 'BPLOT' FOR PLOTTING DATA

```
// JOB
// FOR BPLOT
*VCL PROCESS PROGRAM
*L/CS(CARD,TYPEWRITER,MAGNETIC TAPE,PLOTTER)
*  DOUBLE INTEGERS
      DIMENSION IDTA(600),IDTB(600)
      COMMON IDTA,IDTB ,PA,PI,JTIME,JDAY,JMONT,JSET
C     SWITCH 3 AND 4 NORMALLY DOWN
C     SET SWITCH 3 UP IF DESIRED TO SKIP SOME PLOTS
C     SET SWITCH 4 UP IF DESIRED TO STOP PLOTTING
      DEFINE 4
  100 WRITE(1,15)
   15 FORMAT('PUNCH TIME DATE MONTH SET ,FOR REQD PLOT 14,312')
      CALL BUSY
      READ(2,16)ITIME,IDAY,MONTH,ISET
   16 FORMAT(4A,312)
   25 READ(4)JTIME,JDAY,JMONT,JSET
      IF(JMONT-MONTH) 30,40,30
   40 IF(JDAY-IDAY)30,50,30
   50 IF(JTIME-ITIME)30,60,30
   60 IF(JSET-ISET)30,70,30
   70 READ(4) IDTA,IDTB
      READ(4)JTIME,JDAY,JMONT,JSET
      GO TO 130
   30 READ(4)IDTA,IDTB
      READ(4)JTIME,JDAY,JMONT,JSET
      GO TO 25
  130 WRITE(1,160)
  160 FORMAT('DATA FOR DESIRED PERIOD BEING PLOTTED NOW')
```

```
      K=1
      PI=3.14159
      T=3.*PI/2.
      SX=9./100.
      SY=11./100.
      PX=0.
      PY=0.
      GO TO 1009
    1 CALL
      READ(4)
      READ(4) IDTA,IDTB
      READ(4)JTIME,JDAY,JMONT,JSET
      SX=9./100.
      SY=11./100.
      PX=0.
      PY=0.
 1009 CALL SCALF(SX,SY,PX,PY)
      CALL FCHAR(5.,-40.,.15,.15,F)
      WRITE(7,170)
  170 FORMAT('TIME IN SECS')
      CALL FCHAR(25.,-2.,.15,.15,0.)
      WRITE(7,180)
  180 FORMAT('RECEIVED SIGNAL - DBM')
      CALL FCHAR(1,0.,0.)
 1011 PX=-50.
      PY=200.
      CALL PLOTC
      READ(4)
      READ(4) IDTA,IDTB
      READ(4) JTIME,JDAY,JMONT,JSET
      PX=62.5
      PY=750.
      CALL PLOTC
      READ(4)
      READ(4)JDTA,IDTB
      READ(4) JTIME,JDAY,JMONT,JSET
```

```
      PX=62.5
      PY=750.
      CALL PLOTC
      CALL SSWTCH(3,INDIC)
      GO TO (1002,1006),INDIC
1006  CALL SSWTCH(4,INDIC)
      GO TO (1007,1003),INDIC
1007  WRITE(1,25)
25    FORMAT('PLOTS FOR NEW SET TO BE PLOTTED NOW')
      GO TO 1011
1003  IF(K-2)1004,1005,1004
1004  CALL FPLOT(-2,20.,1700.)
      K=K+1
      READ(4)
      READ(4) IOTA,IDIB
      READ(4) JTIME,JDAY,JMONT,JSET
      GO TO 1011
1005  K=1
      CALL FPLOT(-2,125.,1700.)
      CALL PLOSY
      GO TO 1008
1002  CALL EXIT
      END
```

SUBROUTINE 'PLOTC'

```
// FOR PLOTC
      SUBROUTINE PLOTC
      [illegible] IDTA(600),IDTB(600)
      C[illegible] IDTA,IDTB,PX,PY ,DTLBE,JDAY,JMONT,JSET
      C[illegible] IDTA,IDTB)
      PI=3.14159
      SX=1.25/50.
      SY=2.5/600.
      CALL SCALF(SX,SY,PX,PY)
      CALL FGRID(0,0.,0.,10.,5)
      CALL FGRID(3,0.,0.,100.,6)
      CALL FPLOT(1,0.,0.)
      [illegible]=1
      T=3.*PI/2.
      XD=1.
      X=0.
      Y=100.
      DEL=10.
      XX=0.
      IA=-120
      IMC=10
      DO 200 I=1,6
      IF(ABS(X)-EP)90,70,70
   70 CALL FCHAR(X-XD,Y,.10,.10,T)
      WRITE(7,250)IX
   25 FORMAT(I4)
   90 IX=IX+IMC
      X=X+DEL
  200 CONTINUE
      IY=60
      CALL FCHAR(-5.,-575.,.10,.10,T)
```

```
      WRITE(7,270)II
  270 FORMAT(12)
      CALL PCHAR(50.,-100.,.10,.10,T)
      WRITE(7,280)JTIME,JDAY ,JMONT,JSET,
  280 FORMAT(14,'/',I2,'/',I2,'/',12,'  HOUR=',I1)
      IF(M-2)300,350,350
  300 Y=-1.
      X=IDTA(1)/1637.2
      X=20.*(ALOG(X)/2.303)+32.
      CALL FPLOT(-2,X,Y)
      DO205 M=2,600
      Y=-M
      X=IDTA(M)/1637.2
      X=20.*(ALOG(X)/2.303)+32.
  205 CALL FPLOT(2,X,Y)
      CALL FPLOT(1,0.,0.)
      GX=-62.5
      GY=0.
      CALL SCALF(SX,SY,GX,GY)
      CALL PGRID(0,0.,0.,10.,5)
      CALL PGRID(3,0.,0.,100.,0)
      CALL FPLOT(1,0.,0.)
      Y=-1.
      X=IDTB(1)/1637.2
      X=20.*(ALOG(X)/2.303)+32.
      CALL FPLOT(-2,X,Y)
      DO225 M=2,600
      Y=-M
      X=IDTB(M)/1637.2
      X=20.*(ALOG(X)/2.303)+32.
  225 CALL FPLOT(2,X,Y)
      CALL FPLOT(1,0.,0.)
      N=N+1
      GO TO 401
  350 CALL FPLOT(1,0.,0.)
```

SUBROUTINE 'SHIFT'

```
// FOR SHIFT
      SUBROUTINE SHIFT(IDTA,IDTB)
      DIMENSION IDTA(600),IDTB(500)
      IMIN=IDTA(1)
      DO300 I=2,600
      IF(IDTA(I)-IMIN)200,300,300
  200 IMIN=IDTA(I)
  300 CONTINUE
      DO350 I=1,600
      IF(IDTB(I)-IMIN)250,350,350
  250 IMIN=IDTB(1)
  350 CONTINUE
      IDIF=40-IMIN
      DO400 J=1,600
      IDTB(J)=IDTB(J)+IDIF
  400 IDTA(J)=IDTA(J)+IDIF
      RETURN
      END
```

REFERENCES

1. Panter Philip F., "Communication System Design" McGraw Hill Book Company, p. 343, 1972.

2. Crawford, A.B, D.D. Hogg and W.H. Kummer, "Studies in Tropospheric propogation beyond the horizon", Bell System Tech. Journal, vol. 38, pp. 1067-1178, Sept.,1959.

3. Vogelman, J.H, J.L. Ryerson and M.H. Bickelhaupt, "Tropospheric scatter systems using angle diversity", Proceeding IRE, vol. 47, pp. 688-696, May,1959.

4. Surenian D,, "Experimental results for angle diversity system tests", IEEE Transactions on Communication, vol. COM-13, pp. 208-218, June,1965.

5. Monsen P., "Performance of an experimental angle diversity troposcatter system"", Concise paper, IEEE Trans. in Communication, pp. 242-247, April,1972.

6. Bullington K., "Radio propogation fundamentals", B.S.T.J., vol. 36, pp. 590-626, May,1957.

7. Travais G.W., "Angle Diversity Tests", Proc. NEC, vol. XXIV, pp. 518-523, 1968.

8. Wolff E.A., "Antenna Analysis", John Wiley and Sons, N.Y. Chapters 4&7, 1966.

9. Silver S., "Microwave Antenna theory and design", McGraw Hill, New York, Chapter 12, 1949.

10. Sandler S.S., "Parabolic reflector patterns for off axis feeds", IRE Trans. on Antenna and Propagation, vol. 8, pp. 368-379, July,1960.

11. John Ruze, "Lateral feed displacement in a paraboloid", IEEE Trans. on Antenna and Propagation, vol. 13,pp. 660-665, Sept. 1965.

12. Berkowitz B, "Antennas fed by Horns", Proc. IRE, vol. 41, pp. 1761-1765, Dec., 1953.

13. Rush W.V.T. and Potter P.D. "Analysis of reflector antennas", Academic Press New York, 1970.

14. Jasik H., "Antenna Engineering Handbook", McGraw Hill Book Co., New York, 1961.

15. Swarnakar J.R. Flt.Lt., "A study of effects of feed displacement and reflector antenna deformation on the performance of parabolic reflector antennas", M.Tech. Thesis, Department of Elect. Engg., IIT Kanpur, Aug.,1974.

16. Cutler, "Parabolic antenna design for microwaves', Proc. IRE, vol. 35, Nov., 1947.

17. Skolnik M.I., "Introduction to Radar Systems", McGraw-Hill Book Co. New York, 1962.

18. Blake L.V., "Antennas" John Wiley and Sons.

19. Pande, P.R. Sqn.Ldr., "Qualitative and Quantitative Study of Signal Behaviour for Kanpur-Nainital Troposcatter Link" M.Tech. Thesis, Dept. of Elect. Engg., IIT Kanpur, Aug.1977.

20. Pandey, V.K., "Digital Data Logging System", Technical Report No. TR-02-72, Sept. 1972, ACES, IIT Kanpur.

21. Raju Bh.A.R.B., "The Kanpur Nainital Troposcatter Link, Part II Receiving System", Technical Report No. TR-08-73, Nov. 1973, ACES, IIT Kanpur.

22. Gupta G.C., Sqn.Ldr., "The Kanpur Nainital Troposcatter Link Part III Antenna System", Technical Report No. TR-09-73, Dec.,1973, ACES, IIT Kanpur.

23. Arjun Raman, "The Kanpur Nainital Troposcatter Link, Part I Transmitter", Technical Report No. TR-12-73, Dec.,1973, ACES, IIT Kanpur.

24. Progress Report No. 5, 1st Oct. 73 - 31st March,1974, ACES, IIT Kanpur.

25. Bh.A.R.B. Raju and P.R.K. Rao, "The Kanpur-Nainital Troposcatter Link Data Analysis", Interim Report TR-36-75, Oct.,1975, ACES, IIT Kanpur.

26. Rice, P.L., Longley, A.G. and others 'Transmission loss predictions for tropospheric communication ccts', NBS 101, Volume I, May,1965.

27. I.B.M. 1800 Users' Manual.